How robust are the parameter constraints extending the Λ CDM model?

Stefano Gariazzo,^{1,*} William Giarè,^{2,†} Olga Mena,^{3,‡} and Eleonora Di Valentino^{2,§}

¹Instituto de Fisica Teorica, CSIC-UAM C/ Nicolás Cabrera 13-15,

Campus de Cantoblanco UAM, 28049 Madrid, Spain

²School of Mathematics and Statistics, University of Sheffield,

Hounsfield Road, Sheffield S3 7RH, United Kingdom

³Instituto de Física Corpuscular (CSIC-Universitat de València), E-46980 Paterna, Spain

(Dated: April 18, 2024)

We present model-marginalized limits on the six standard Λ CDM cosmological parameters ($\Omega_c h^2$, $\Omega_{\rm b}h^2$, $\theta_{\rm MC}$, $\tau_{\rm reio}$, n_s and A_s), as well as on selected derived quantities $(H_0, \Omega_{\rm m}, \sigma_8, S_8 \text{ and } r_{\rm drag})$, obtained by considering three independent Cosmic Microwave Background (CMB) experiments: the Planck satellite, the Atacama Cosmology Telescope, and South Pole Telescope. We also consider low redshift observations in the form of Baryon Acoustic Oscillation (BAO) data from the SDSS-IV eBOSS survey and Supernovae (SN) distance moduli measurements from the Pantheon-Plus catalog. The marginalized errors are stable against the different fiducial cosmologies explored in this study. The largest impact on the parameter accuracy is produced by varying the effective number of relativistic degrees of freedom (N_{eff}) or the lensing amplitude (A_{lens}) . Nevertheless the marginalized errors on some derived parameters such as H_0 or $\Omega_{\rm m}$ can be up to two orders of magnitude larger than in the canonical ΛCDM scenario when considering only CMB data. In these cases, low redshift measurements are crucial for restoring the stability of the marginalized cosmological errors computed here. Overall, our results underscore remarkable stability in the mean values and precision of the main cosmological parameters, making irrelevant the choice of different possible cosmological scenarios once both high and low redshift probes are fully accounted for. The very same results should be understood as a tool to test exotic cosmological scenarios, as the marginalized values should be used in numerical analyses due to their robustness and slightly larger errors, providing a more realistic and conservative approach.

I. INTRODUCTION

The minimal Λ CDM model of cosmology has successfully explained a large number of cosmological observations at different scales. Within this minimal theoretical framework, the complexity of the Cosmic Microwave Background (CMB) acoustic peak structure or the matter power spectrum can be well described by only six fundamental parameters: the cold dark matter density $(\Omega_{\rm c}h^2)$, the baryon density $(\Omega_{\rm b}h^2)$, the angular size of the sound horizon at recombination ($\theta_{\rm MC}$), the optical depth (τ_{reio}) , and the inflationary parameters such as the spectral index (n_s) and the amplitude (A_s) of scalar perturbations. Starting from these six parameters, a number of other important (derived) quantities can be computed, including the Hubble constant (H_0) , the matter density $(\Omega_{\rm m})$, the clustering parameters (σ_8) and $S_8 \equiv \sigma_8 \sqrt{\Omega_{\rm m}/0.3}$), or the sound horizon at the drag epoch $r_{\rm drag}$.

Given the robustness and resilience shown in the results obtained over the years from different CMB experiments and large-scale structure probes, the mean values and errors of these parameters are often used to fit more exotic cosmological scenarios. For instance, the

values of σ_8 and/or $r_{\rm drag}$ have been extensively used in the literature to test modified gravity models, interacting cosmologies, cosmologies with additional degrees of freedom, or non-standard neutrino scenarios. Nevertheless, it should be noted that the fitting values and uncertainties of these (primary and derived) quantities are obtained within some precise theoretical assumptions. In spite of the remarkable success and the simplicity of our best-working model of the universe, there is solid ground to believe that some missing physics phenomena are absent in Λ CDM. The most obvious example concerns neutrino masses: from neutrino oscillation experiments, we know that neutrinos are not massless; however, their total mass, required to be within the sub-eV regime, is totally unknown. While neutrinos should be massive, there could be additional missing ingredients in this minimal recipe of our universe. Just to mention a few concrete examples, dark energy could not be as simple as a cosmological constant (see, for instance, the indication at 3.9σ for Dynamical Dark Energy as obtained by the recent DESI release [1]) or there could be a small curvature component in our universe, as seems to be indicated by some analyses of the CMB measurements from the Planck 2018 legacy release with the baseline Plik likelihood [2], which seem to point towards the possibility of a closed Universe at more than three standard deviations [3–7].

As a result, one straightforward question is how stable the mean values and errors of the main cosmological parameters (including the derived ones) describing the minimal Λ CDM scenario are. Answering this question is of primary importance because robustness in their mean

^{*} stefano.gariazzo@ift.csic.es

 $^{^{\}dagger}$ w.giare@sheffield.ac.uk

[‡] omena@ific.uv.es

[§] e.divalentino@sheffield.ac.uk

values and errors is absolutely required to test exotic cosmological scenarios. Therefore, a stable and robust estimation of these parameters constitutes a unique tool for cosmological analyses.

In this manuscript, we address the issue raised above by computing the marginalized errors on the main cosmological parameters over a range of possible fiducial cosmologies (see Refs. [8–11] for previous studies dealing with such a marginalization procedure). Therefore, we not only provide an answer regarding the stability of our current (minimal) description of the universe but also offer a set of robust mean values and errors that can be used as input when testing different non-standard physical scenarios.

The manuscript is organized as follows. Sec. II describes the methodology of the marginalization procedure, the data used in the analyses, and the different fiducial cosmologies included in the marginalization. Sec. III presents our results, which include tables and figures illustrating the deviation from the expected values within the different fiducial cosmologies. We conclude in Sec. IV.

II. METHODOLOGY

A. Basic statistics

In the following, we shall review the basics of Bayesian statistics necessary for performing a marginalization over a number of different models. We refer the reader to Refs. [8–11] for a more complete description of the full statistical analysis.

Given a set of possible models \mathcal{M}_i with prior probabilities π_i , we begin by computing their Bayesian evidences Z_i for the selected dataset d. The posterior probability of model i over all possible models, p_i , can be computed using:

$$p_i = \frac{\pi_i Z_i}{\sum_j \pi_j Z_j} \,. \tag{1}$$

If all models share a parameter or set of parameters θ , we can use the model posterior probabilities p_i together with the parameter posterior probability within model i, $p(\theta|d, \mathcal{M}_i)$, to compute the model-marginalized posterior probability $p(\theta|d)$ for θ , given some data d:

$$p(\theta|d) \equiv \sum_{i} p(\theta|d, \mathcal{M}_i) p_i$$
. (2)

If all models have the same prior and using the Bayes factors $B_{i0} = Z_i/Z_0$ with respect to the favored model \mathcal{M}_0 , the model-marginalized posterior becomes:

$$p(\theta|d) = \frac{\sum_{i} p(\theta|d, \mathcal{M}_i) B_{i0}}{\sum_{j} B_{j0}}.$$
 (3)

Notice that if the Bayes factors are large in favor of the preferred model (usually the simplest one), extensions of the minimal picture will not contribute significantly to the model-marginalized posterior.

In order to perform Bayesian model comparison using the Bayes factors and evaluate the strength of preference in favor of the best model, we follow a modified version of the Jeffreys' scale¹ extracted from Ref. [13], see Tab. I.

B. Theoretical Models

As pointed out in the introduction, a key point in our analysis is to derive robust bounds on the basic six Λ CDM cosmological parameters and a number of derived ones $(H_0, \, \Omega_{\rm m}, \, \sigma_8, \, S_8 \,$ and $r_{\rm drag})$ by marginalizing over a plethora of possible background cosmologies. We recall here that $S_8 \equiv \sigma_8 \sqrt{\Omega_{\rm m}/0.3}$ and $r_{\rm drag}$ is the sound horizon at the baryon drag epoch, the comoving distance a wave can travel prior to $z_{\rm drag}$, when baryons and photons decouple.

Therefore, along with the six Λ CDM parameters, we also include several extensions of this minimal model, enlarging the parameter space including one or more degrees of freedom, such as a running of the scalar spectral index (α_s) , a curvature component (Ω_k) , the dark energy equation of state – either parameterized via one single parameter (w_0) , or via two parameters (w_0) and $w_a)$ – the total neutrino mass $(\sum m_{\nu})$, the effective number of relativistic degrees of freedom $(N_{\rm eff})$, and the lensing amplitude $(A_{\rm lens})$. A short description of each parameter follows.

- The running of scalar spectral index, α_s . In simple inflationary models, the running of the spectral index is typically very small. However, specific models can produce a large running over a range of scales accessible to CMB experiments. Indeed, a non-zero value of α_s alleviates the $\sim 2.7\sigma$ discrepancy in the value of the scalar spectral index n_s measured by Planck ($n_s = 0.9649 \pm 0.0044$) [14] and by the $Atacama\ Cosmology\ Telescope\ (ACT)$ ($n_s = 1.008 \pm 0.015$) [15], see Refs. [16–18]. ACT and Planck are actually in tension regarding the estimate of α_s (see Ref. [19]).
- Curvature density, Ω_k . Recent data analyses of the CMB temperature and polarization spectra from Planck 2018 team exploiting the baseline *Plik* likelihood suggest that our Universe could have a closed geometry at more than three standard deviations [4, 5, 14, 20]. These hints mostly arise from TT observations, that would otherwise show a lensing excess [6, 21, 22]. In addition, analyses exploiting the *CamSpec* TT likelihood [23, 24] point

¹ Notice that our empirical scale, summarized in Tab.I, deviates from the scale defined in the original Jeffreys' work [12])

$ \ln B_0 $	Odds	Probability	Strength of evidence
< 0.1	$\lesssim 3:1$	< 0.750	Inconclusive
1	$\sim 3:1$	0.750	Weak
2.5	$\sim 12:1$	0.923	Moderate
5	$\sim 150:1$	0.993	Strong

Table I: Modified Jeffreys' empirical scale to establish the strength of evidence when comparing two competing models.

Parameter	Prior
$\Omega_{ m b}h^2$	[0.005,0.1]
$\Omega_{ m c} h^2$	[0.001,0.99]
$\log(10^{10}A_{\rm S})$	[2.91,3.91]
$n_{ m s}$	[0.8,1.2]
$100 heta_{ m MC}$	[0.5,10]
au	0.065 ± 0.015
Ω_{k}	[-0.3,0.3]
w_0	[-3,1]
w_a	[-3,2]
$lpha_{ m s}$	[-1,1]
$\sum m_{\nu} \text{ [eV]}$	[0.06,5]
$N_{ m eff}$	[0.05,10]
$A_{\rm lens}$	[0, 5]

Table II: List of uniform prior distributions for cosmological parameters.

to a closed geometry of the Universe with a significance above 99% CL. However, this indication is reduced with the new *HiLLiPoP* likelihood [25]. Furthermore, an indication for a closed universe is also present in the BAO data, using Effective Field Theories of Large Scale Structure [26]. These recent findings strongly motivate to leave the curvature of the Universe as a free parameter [27] and obtain marginalized limits on the different cosmological parameters, accounting also for this context.

• Dark Energy equation of state, w_0 or w_0w_a . Cosmological bounds become weaker if the dark energy equation of state is taken as a variable quantity. Indeed, the dark energy equation of state, not that associated to a cosmological constant Λ , has non-trivial degeneracies with a number of cosmological parameters, such as the Hubble constant or the total matter density. Even if current data fits well with the assumption of a cosmological constant

within the minimal Λ CDM scenario² (except in the case of DESI observations [1]) the question of having an equation of state parameter different from -1 remains certainly open. Along with constant dark energy equation of state models, in this paper we also consider the possibility of having a time-varying w(a) described by the Chevalier-Polarski-Linder parametrizazion (CPL) [29, 30]:

$$w(a) = w_0 + (1 - a)w_a (4)$$

where a is the scale factor and is $a_0 = 1$ at the present time, $w(a_0) = w_0$ is the value of the equation of state parameter today. Dark energy changes the distance to the CMB consequently pushing it further (closer) if w < -1 (w > -1) from us. This effect can be balanced, for instance, by having a different matter density or a shifted value of H_0 .

- Neutrino mass, $\sum m_{\nu}$. Current cosmological data from the Planck CMB satellite, the SDSS-III and SDSS-IV galaxy clustering surveys [31, 32] and the Pantheon Supernova Ia provides the most constraining neutrino mass bound to date, $\sum m_{\nu}$ < 0.09 eV at 95% CL [33], mostly due to Redshift Space Distortions analyses from the SDSS-IV eBOSS survey (see also Ref. [34] for a very competitive limit), implying that six million neutrinos cannot weigh more than one electron. More recently, the DESI collaboration reported a even stronger limit $\sum m_{\nu} < 0.072$ (0.113) eV at 95% CL if the prior on the sum of the neutrino masses is assumed to be $\sum m_{\nu} \geq 0 \ (0.059) \text{ eV} \ [1]$. A larger amount of neutrino masses will shift the Hubble parameter towards smaller values. The value of the current matter energy density will be larger. This will also have a non-negligible impact in the value of the clustering parameter σ_8 .
- The effective number of relativistic degrees of freedom, $N_{\rm eff}$. Our current knowledge of the relativistic degrees of freedom at decoupling demonstrates that $N_{\rm eff}$ is close to 3 as measured by CMB observations ($N_{\rm eff}=2.99^{+0.34}_{-0.33}$ at 95% confidence level (CL)

² See also recent Ref. [28] for a review on the constraints on the Dark Energy equation of state resulting from different cosmological and astrophysical data.

- [14]) or BBN abundances (e.g. $N_{\rm eff}=2.87^{+0.24}_{-0.21}$ at 68% CL [35]) independently. A larger value of $N_{\rm eff}$ will imply more radiation in the early universe and will be degenerate with the matter density, the amplitude of the primordial power spectrum and the Hubble constant.
- The lensing amplitude, A_{lens} . CMB anisotropies get blurred due to gravitational lensing by the large scale structures of the Universe: photons from different directions are mixed and the peaks at large multipoles are smoothed. The amount of lensing within a given cosmology can be changed by means of the factor A_{lens} [21], the so-called lensing amplitude and, a priori, an unphysical parameter. Within the minimal Λ CDM scenario, $A_{lens} = 1$. Planck measurements of the CMB temperature and polarization indicate that data shows a preference for additional lensing, suggesting $A_{lens} > 1$ at 3σ . CMB lensing can be also extracted from CMB observations via a four-point correlation function. If this independent measurement is added the tension is ameliorated, albeit it is still above the canonical one by about 2σ . This lensing anomaly could have its origin in other physics effects unrelated to lensing. Also in this case, this indication is reduced with the new Hillipop likelihood [25]. The lensing amplitude also shows non-negligible degeneracies with a number of cosmological parameters, as for instance, with the dark matter mass-energy density or with the reionization optical depth $\tau_{\rm reio}$ [36].

C. Statistical Analyses and Likelihoods

Our statistical analysis of CMB and large scale structure probes is based on the public code COBAYA [37], of which we make use of the Monte Carlo Markov Chain (MCMC) sampler, originally developed for CosmoMC [38]. The sampler allows to perform parameter space exploration with speed hierarchy implementing the "fast dragging" procedure developed in [39]. The prior distributions for the parameters involved in our analysis are chosen to be uniform along the range of variation (see Tab. II) with the exception of the optical depth for which the prior distribution is chosen accordingly to the CMB datasets as discussed below. From the MCMC results, we compute Bayesian evidences thanks to the publicly available package MCEvidence, properly modified to be compatible with COBAYA. It has been shown in the past, see e.g. [10, 11], that the MCEvidence algorithm can accurately reproduce the Bayes factors obtained with nested sampling tools such as PolyChord [42, 43], but with shorter computation time. A reasonable estimate

of the numerical uncertainties on the Bayes factors obtained here is therefore $\sigma(\log B) \sim 0.5$ [10].

Concerning the cosmological and astrophysical observations, our baseline data-sets and likelihoods include:

- Planck 2018 temperature and polarization (plik TT TE EE) likelihoods, which also include low multipole data (\(\ell < 30\)) [3, 44, 45], in combination with the Planck 2018 lensing likelihood [46], reconstructed from measurements of the power spectrum of the lensing potential. This dataset is referred to as *Planck*.
- Atacama Cosmology Telescope temperature and polarization anisotropy DR4 likelihood, in combination with the gravitational lensing DR6 likelihood covering 9400 deg² reconstructed from CMB measurements made by the Atacama Cosmology Telescope from 2017 to 2021 [47, 48]. In our analysis for the lensing spectrum we include only the conservative range of lensing multipoles $40 < \ell < 763$. We consider a Gaussian prior on $\tau = 0.065 \pm 0.015$, as prescribed in [15]. We refer to this dataset as ACT.
- South Pole Telescope temperature and polarization (TT TE EE) likelihood [49]. Also in this case we consider a Gaussian prior on $\tau = 0.065 \pm 0.015$, We refer to this dataset as SPT.
- Local Universe observations in the form of
 - i) Baryon Acoustic Oscillation data from the finalized SDSS-IV eBOSS survey. These data encompass both isotropic and anisotropic distance and expansion rate measurements, as outlined in Table 3 of Reference [50].
 - ii) Distance modulus measurements of Type Ia supernovae obtained from the *Pantheon-Plus* sample [51]. This dataset comprises 1701 light curves representing 1550 unique Type Ia supernovae, spanning a redshift range from 0.001 to 2.26.

We will refer to the combination of these two likelihoods as *low-z*.

III. RESULTS

Tab. III and IV depict the marginalized constraints (respectively at 68 and 95% CL) on the different cosmological parameters explored here arising from the different data sets. The bounds derived within each of the fiducial cosmologies described in the previous section are shown in Tabs. V-XII, which also include the minimal ΛCDM scenario.

A. Base Λ CDM parameters

Let us start commenting on the baryon mass-energy density, $\Omega_{\rm b}h^2$. Figure 1 illustrates the shift in the one-

 $^{^3}$ github.com/yabebal Fantaye/MCE
vidence [40, 41].

Parameter	Planck	ACT	SPT	$ ule{blanck+low-z}$	ACT+low-z	$\operatorname{SPT+low-}z$
$\Omega_{ m b} h^2$	$0.02240^{+0.00015}_{-0.00016}$	$0.02147^{+0.00039}_{-0.00043}$	$0.02220^{+0.00033}_{-0.00032}$	$0.02242^{+0.00015}_{-0.00013}$	0.02147 ± 0.00034	0.02223 ± 0.00032
$\Omega_{ m c} h^2$	$0.1197^{+0.0013}_{-0.0015}$	$0.1187^{+0.0040}_{-0.0062}$	$0.1171^{+0.0059}_{-0.0048}$	$0.11925^{+0.0010}_{-0.00098}$	0.1189 ± 0.0017	$0.1178^{+0.0024}_{-0.0023}$
$100\theta_{\mathrm{MC}}$	1.04095 ± 0.00032	$1.04227^{+0.00084}_{-0.00080}$	$1.04009^{+0.00081}_{-0.00079}$	$1.04101^{+0.00029}_{-0.00030}$	1.04219 ± 0.00065	
$ au_{ m reio}$	$0.0529^{+0.0080}_{-0.0073}$	0.064 ± 0.015	0.061 ± 0.015	$0.0565^{+0.0075}_{-0.0069}$	$0.066^{+0.013}_{-0.011}$	$0.063^{+0.014}_{-0.013}$
$n_{ m s}$	$0.9658^{+0.0044}_{-0.0045}$	$0.990^{+0.017}_{-0.031}$	$0.966^{+0.021}_{-0.022}$	$0.9670^{+0.0036}_{-0.0040}$	$0.990^{+0.014}_{-0.023}$	$0.969^{+0.020}_{-0.017}$
$\log(10^{10}A_{\rm s})$	3.041 ± 0.016	$3.050^{+0.034}_{-0.032}$	$3.054^{+0.035}_{-0.032}$	$3.048^{+0.015}_{-0.014}$	$3.061^{+0.024}_{-0.025}$	3.061 ± 0.029
$H_0 [\mathrm{km/s/Mpc}]$		$67.2^{+6.1}_{-10}$	$68.3^{+19}_{-4.0}$	$67.64^{+0.49}_{-0.41}$	$67.33^{+0.66}_{-0.60}$	$67.84^{+0.67}_{-0.78}$
$\Omega_{ m m}$	$0.315^{+0.052}_{-0.016}$	$0.313^{+0.048}_{-0.024}$	$0.296^{+0.093}_{-0.14}$	$0.3104^{+0.0059}_{-0.0051}$	$0.3116^{+0.0061}_{-0.0072}$	$0.3056^{+0.0094}_{-0.0082}$
σ_8	$0.810^{+0.24}_{-0.026}$	$0.830^{+0.033}_{-0.074}$	$0.804^{+0.067}_{-0.21}$	$0.811^{+0.014}_{-0.015}$	$0.8322^{+0.0088}_{-0.0095}$	0.811 ± 0.014
S_8	$0.832^{+0.030}_{-0.025}$	0.848 ± 0.025	$0.789^{+0.063}_{-0.073}$	$0.827^{+0.011}_{-0.012}$	0.847 ± 0.013	0.821 ± 0.019
$r_{\rm drag} \ [{ m Mpc}]$	147.16 ± 0.31	$148.38^{+1.1}_{-0.98}$	$147.9^{+1.2}_{-1.7}$	$147.24^{+0.30}_{-0.32}$	$148.38^{+0.69}_{-0.66}$	$147.85^{+0.68}_{-0.72}$

Table III: Mean values and 68% CL errors on the six Λ CDM parameters as well as on some derived ones (H_0 , $\Omega_{\rm m}$, σ_8 , S_8 , $r_{\rm drag}$ and $D_{\rm A}$) after marginalizing over a complete and large number of possible fiducial cosmologies. We illustrate the results from Planck, ACT and SPT CMB observations, either alone or combined with low redshift measurements.

Parameter	Planck	ACT	SPT	Planck+low-z	$ ext{ACT+low-}z$	$\operatorname{SPT+low-}z$
$\Omega_{ m b} h^2$		-0.0010	$0.02220^{+0.00066}_{-0.00064}$	$0.02242^{+0.00028}_{-0.00026}$	$0.02147^{+0.00065}_{-0.00068}$	$0.02223^{+0.00066}_{-0.00061}$
$\Omega_{\rm c} h^2$	$0.1197^{+0.0026}_{-0.0031}$	$0.1187^{+0.0059}_{-0.016}$	$0.1171^{+0.013}_{-0.0089}$	0.1192 ± 0.0025	$0.1189^{+0.0033}_{-0.010}$	$0.1178^{+0.016}_{-0.0041}$
$100\theta_{\mathrm{MC}}$	$1.04095^{+0.00064}_{-0.00062}$	$1.0423^{+0.0019}_{-0.0015}$	1.0401 ± 0.0016	$1.04101^{+0.00058}_{-0.00059}$	$1.0422^{+0.0014}_{-0.0013}$	$1.0402^{+0.0014}_{-0.0015}$
$ au_{ m reio}$	$0.053^{+0.016}_{-0.015}$	0.064 ± 0.029	0.061 ± 0.029	$0.057^{+0.015}_{-0.014}$	$0.066^{+0.025}_{-0.023}$	$0.063^{+0.027}_{-0.026}$
$n_{ m s}$	$0.9658^{+0.0093}_{-0.0089}$	$0.990^{+0.033}_{-0.062}$	$0.966^{+0.048}_{-0.047}$	$0.9670^{+0.0075}_{-0.0079}$	$0.990^{+0.027}_{-0.039}$	$0.969^{+0.053}_{-0.033}$
$\log(10^{10}A_{\rm s})$	$3.041^{+0.032}_{-0.033}$	$3.050^{+0.063}_{-0.069}$	$3.054^{+0.071}_{-0.064}$	$3.048^{+0.030}_{-0.029}$	$3.061^{+0.045}_{-0.049}$	$3.061^{+0.057}_{-0.058}$
$H_0 [\mathrm{km/s/Mpc}]$	$67.3^{+33}_{-6.9}$	67^{+33}_{-10}	68^{+28}_{-18}	$67.64^{+1.1}_{-0.95}$	$67.3^{+1.3}_{-2.9}$	$67.8^{+4.0}_{-1.5}$
Ω_{m}	$0.315^{+0.077}_{-0.17}$	$0.31^{+0.11}_{-0.17}$	$0.30^{+0.33}_{-0.15}$	0.310 ± 0.011	0.312 ± 0.013	$0.306^{+0.015}_{-0.013}$
σ_8	$0.810^{+0.25}_{-0.034}$	$0.830^{+0.25}_{-0.095}$	$0.80^{+0.12}_{-0.28}$	$0.811^{+0.014}_{-0.015}$	$0.832^{+0.018}_{-0.022}$	$0.811^{+0.034}_{-0.027}$
S_8	$0.832^{+0.049}_{-0.096}$	$0.848^{+0.051}_{-0.086}$	$0.79^{+0.13}_{-0.16}$	$0.827^{+0.021}_{-0.023}$	$0.847^{+0.025}_{-0.026}$	$0.821^{+0.040}_{-0.037}$
$r_{\rm drag} \ [{ m Mpc}]$	$147.16^{+0.85}_{-0.78}$	$148.4^{+3.6}_{-1.6}$	$147.9^{+2.3}_{-3.3}$	$147.2^{+2.1}_{-1.9}$	$148.4^{+3.6}_{-1.3}$	$147.8^{+1.3}_{-3.8}$

Table IV: As Tab. III but with 95% CL marginalized bounds.

dimensional posterior probability for $\Omega_b h^2$ arising from all the fiducial cosmologies and all data combinations, including also the marginalized distributions. Notice firstly that the largest departure in the uncertainty of $\Omega_{\rm b}h^2$ from its reference value within the Λ CDM cosmology occurs when either N_{eff} or A_{lens} are free parameters, being twice as large for the effective number of neutrino species. This was somehow expected, as the baryon mass energy density is measured from observations of the relative height of the second CMB peak with respect to the first and third peaks: if one adds baryons, the odd peaks are enhanced over the even peaks, that is, baryons make the first acoustic peak much larger than the second. The more baryons, the more the second peak is relatively suppressed, as the extra gravity provided by the baryons will enhance the compression into the potential wells. On the other hand, a larger $N_{\rm eff}$ will mostly affect the CMB power spectrum at high multipoles ℓ , rather than at the very first peaks, i.e. at the CMB damping tail [52]. If $\Delta N_{\rm eff}$ increases, the Hubble parameter H during radiation domination will increase as well. Baryon-photon decoupling is not an instantaneous process, leading to a diffusion damping of oscillations in the plasma. If decoupling starts at $\tau_{\rm d}$ and ends at $\tau_{\rm ls}$, during $\Delta \tau$ the radiation free streams on scale $\lambda_d = (\lambda \Delta \tau)^{1/2}$ where λ is the photon mean free path and λ_d is shorter than the thickness of the last scattering surface. As a consequence, temperature fluctuations on scales smaller than λ_d are damped, because on such scales photons can spread freely both from overdensities and underdensities. The overall result is that the damping angular scale $\theta_{\rm d} = r_{\rm d}/D_{\rm A}$ is proportional to the square root of the expansion rate $\theta_{\rm d} \propto \sqrt{H}$ and consequently it increases with $\Delta N_{\rm eff}$, inducing a suppression of the peaks located at high multipoles and a smearing of the oscillations that intensifies at the CMB damping tail. Therefore, when considering N_{eff} as a free parameter, the bounds on the baryon energy density are loosened as they affect the CMB anisotropies in nearby multipole regions. A similar situation, albeit to a minor extent, happens with the lensing amplitude A_{lens} . CMB temperature fluctuations get blurred due to gravitational lensing by the large scale structure of the Universe: photons from different directions are mixed and the peaks at large multipoles are smoothed. The amount of lensing is a precise prediction of the Λ CDM model: the consistency of the model can be checked by artificially increasing lensing by a factor A_{lens} [21] (a priori an unphysical parameter). If Λ CDM consistently describes all

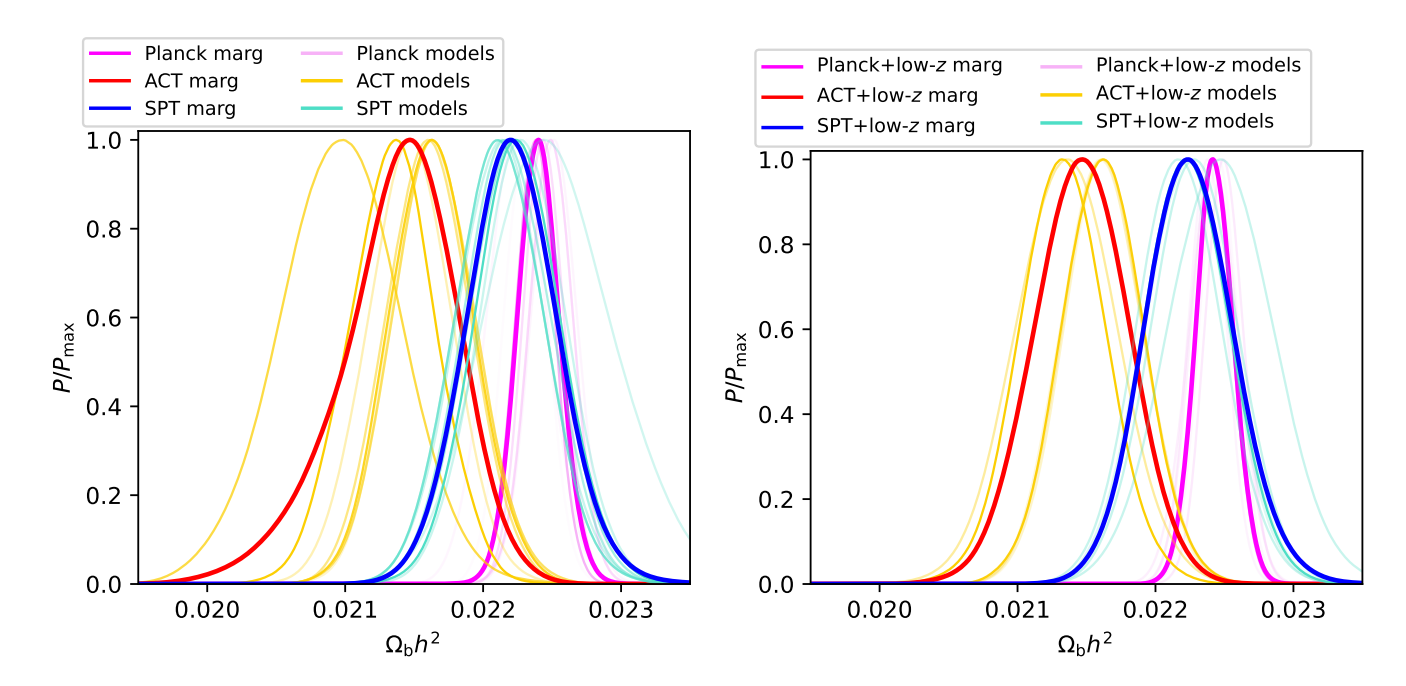


Figure 1: Marginalized 1D posteriors for $\Omega_b h^2$, considering different datasets. Lighter colors (pink for Planck, yellow for ACT, light blue for SPT) indicate the posteriors for each of the various cosmological models, where the least favorite models correspond to fainter lines. The model-marginalized posteriors are shown in brighter colors (magenta for Planck, red for ACT, blue for SPT). The left (right) panel represents results obtained without (with) low-z data.

CMB data, observations should prefer $A_{\rm lens}=1.$ Since the effect of the lensing amplitude is also focused in the large multipoles peaks, it partly affects the extraction of $\Omega_{\rm b}h^2$. These larger uncertainties in $\Omega_{\rm b}h^2$ are observed in case of Planck, ACT and SPT data. Once low redshift measurements are accounted for, the uncertainties are reduced and are much closer to the standard ΛCDM ones. Indeed, the marginalized errors on $\Omega_b h^2$ depicted in Tab. IV are very close to the Λ CDM ones, see Tab. V. Figure 1 shows that effect: the spread in the mean values of $\Omega_{\rm b}h^2$ for ACT and SPT is reduced when low-z data are added in the numerical analyses. It also shows that the mean value preferred by ACT is lower than that preferred by SPT or Planck, showing a (mild) $\sim 2\sigma$ discrepancy. Interestingly, this mismatch does not dilute when adding low-redshift observations. The reason for that is due to the higher CMB second peak amplitude preferred by ACT measurements when compared to Planck observations, implying therefore a lower baryon mass energy density with respect to that preferred by Planck data.

The following parameter to be discussed is the dark matter mass energy density. Figure 2 depicts the marginalized 1D posteriors for $\Omega_{\rm c}h^2$, considering different datasets. As in the case of $\Omega_{\rm b}h^2$, the largest departure from the canonical $\Lambda{\rm CDM}$ theory is also reached when either $N_{\rm eff}$ or $A_{\rm lens}$ are free parameters in the fiducial cosmology. Indeed, the degeneracy with $N_{\rm eff}$ can be easily understood in terms of the early Integrated Sachs Wolfe (ISW) effect. This effect is originated from the interaction between CMB photons and the time-dependent

gravitational potentials along the line of sight between us and the last scattering surface. Notice that the early ISW effect adds in phase with the primary anisotropy, increasing the height of the first acoustic peaks, with an emphasis on the first one, where the main contribution of the ISW effect lies. In addition, the early ISW effect will be suppressed by the square of the radiation-to-matter ratio $\propto [(1+z_{\rm r})/(1+z_{\rm eq})]^2$, i.e. a larger (smaller) matter component will result into a smaller (larger) ISW amplitude due to the larger (smaller) value of z_r . Conversely, a larger (smaller) amount of radiation – i.e. larger (smaller) $N_{\rm eff}$ – will result into a larger (smaller) ISW effect. This is also the reason for the lower value of $\Omega_{\rm c}h^2$ preferred by ACT observations, due to their slightly different amplitude of the first CMB acoustic peak when compared to Planck data. Concerning A_{lens} , notice that there is always a preference for $A_{\rm lens} > 1$ when considering Planck or SPT data, see Tab. X. This implies more CMB lensing and to compensate for that a lower matter density would be required. In the case of SPT, however, we find a value of $A_{\rm lens} < 1$, and therefore the value of $\Omega_{\rm c} h^2$ will be higher than in the standard Λ CDM picture. Finally, the marginalized constraints on the dark matter energy density are very close to those obtained within the minimal scenario, reassuring the stability of the main cosmological parameters, despite the fact that also a timedependent dark energy equation of state, parameterized via the CPL prescription, or a non-zero curvature, will also have a non-negligible impact on $\Omega_c h^2$, see Tabs. XII and IX.

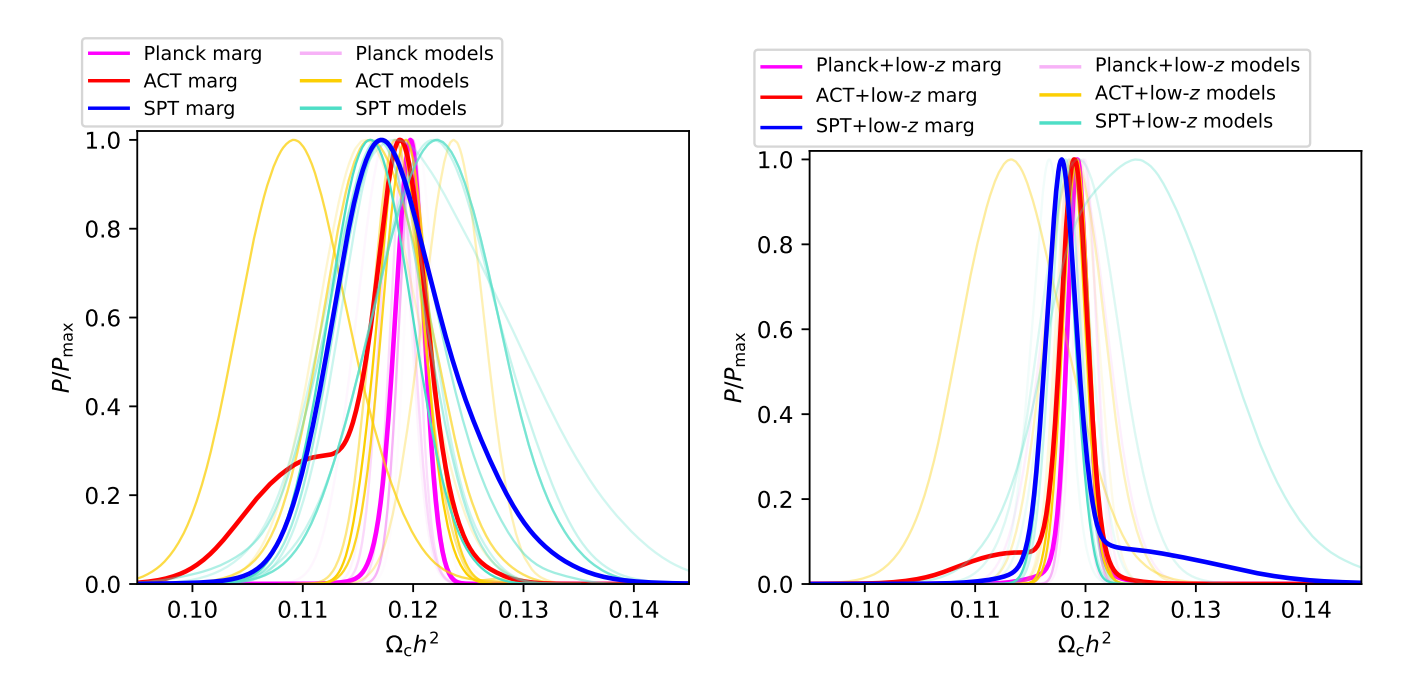


Figure 2: Marginalized 1D posteriors for $\Omega_c h^2$, considering different datasets. Colors are the same as in Fig. 1.

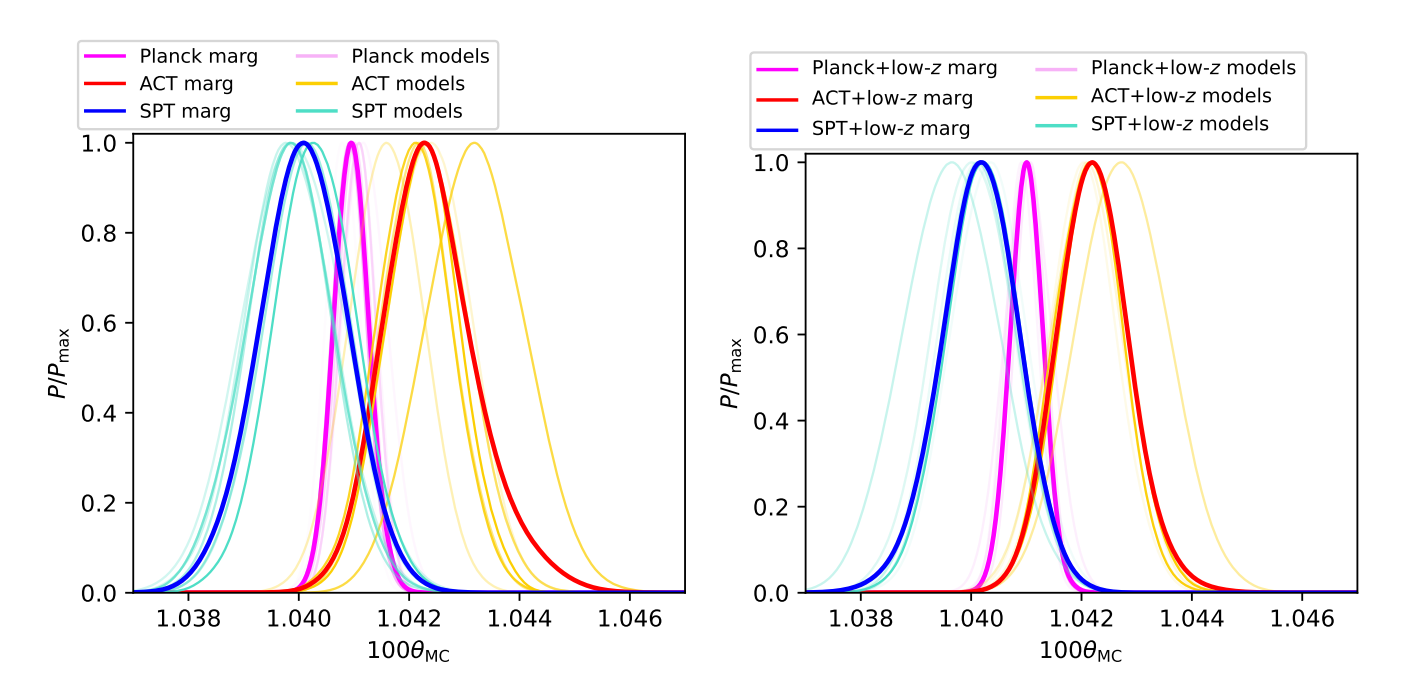


Figure 3: Marginalized 1D posteriors for $100\theta_{\rm MC}$, considering different datasets. Colors are the same as in Fig. 1.

The next parameter we shall discuss is $\theta_{\rm MC}$, an approximation to the angular scale of the sound horizon at decoupling, based on some model-dependent analytical fits. In Figs. 3 we depict the one-dimensional probability distributions for this parameter. Table IV shows the marginalized constraints on $100\theta_{\rm MC}$. The very first thing to notice is that this parameter is very well constrained by Planck CMB measurements, while higher multipole

damping-tail CMB probes, such as SPT or ACT, lead to much larger errors. This is due to the fact that Planck observations have an extremely good accuracy around the first acoustic peaks while ACT and SPT are focused on the high multipole region, where it is more difficult to determine the angular position of the peaks because of their smaller amplitudes. Notice as well that low redshift observations from BAO data do not improve much

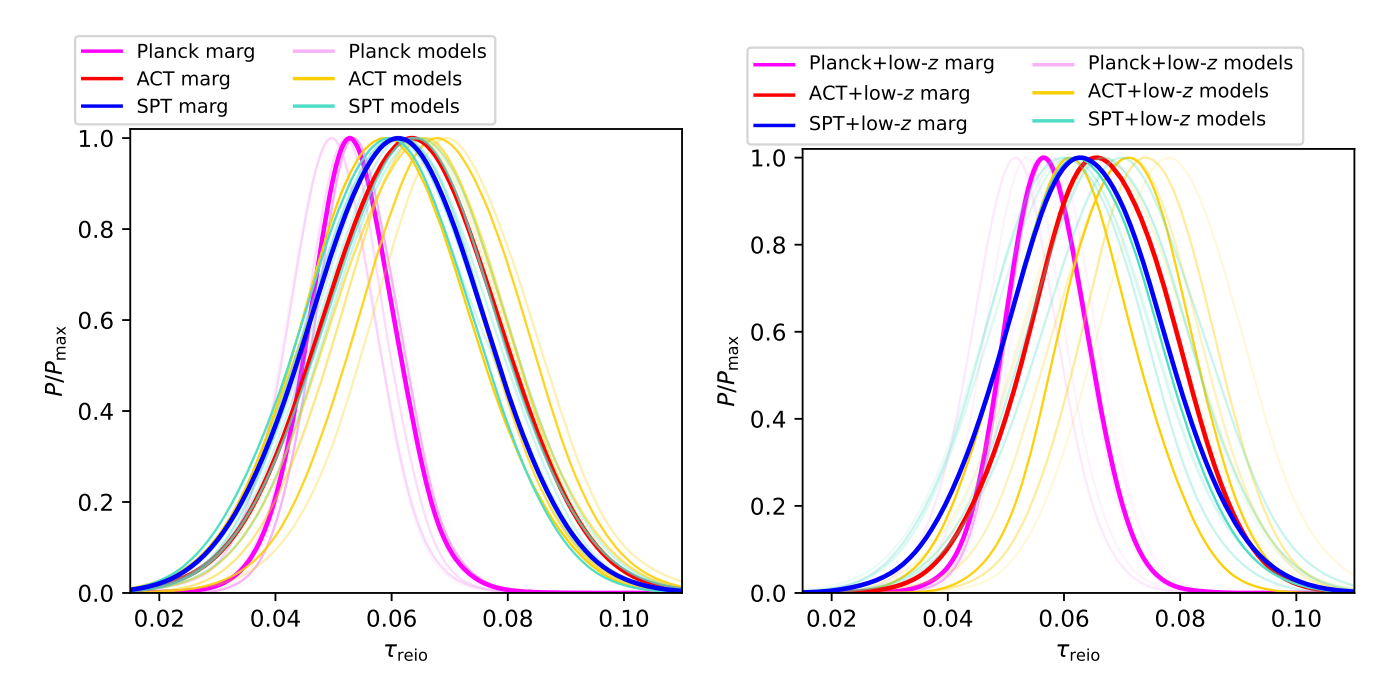


Figure 4: Marginalized 1D posteriors for $\tau_{\rm reio}$, considering different datasets. Colors are the same as in Fig. 1. In the ACT and SPT cases we are assuming a Gaussian prior, so these two experiments are not sensitive to $\tau_{\rm reio}$ and we are re-obtaining the prior used as an input.

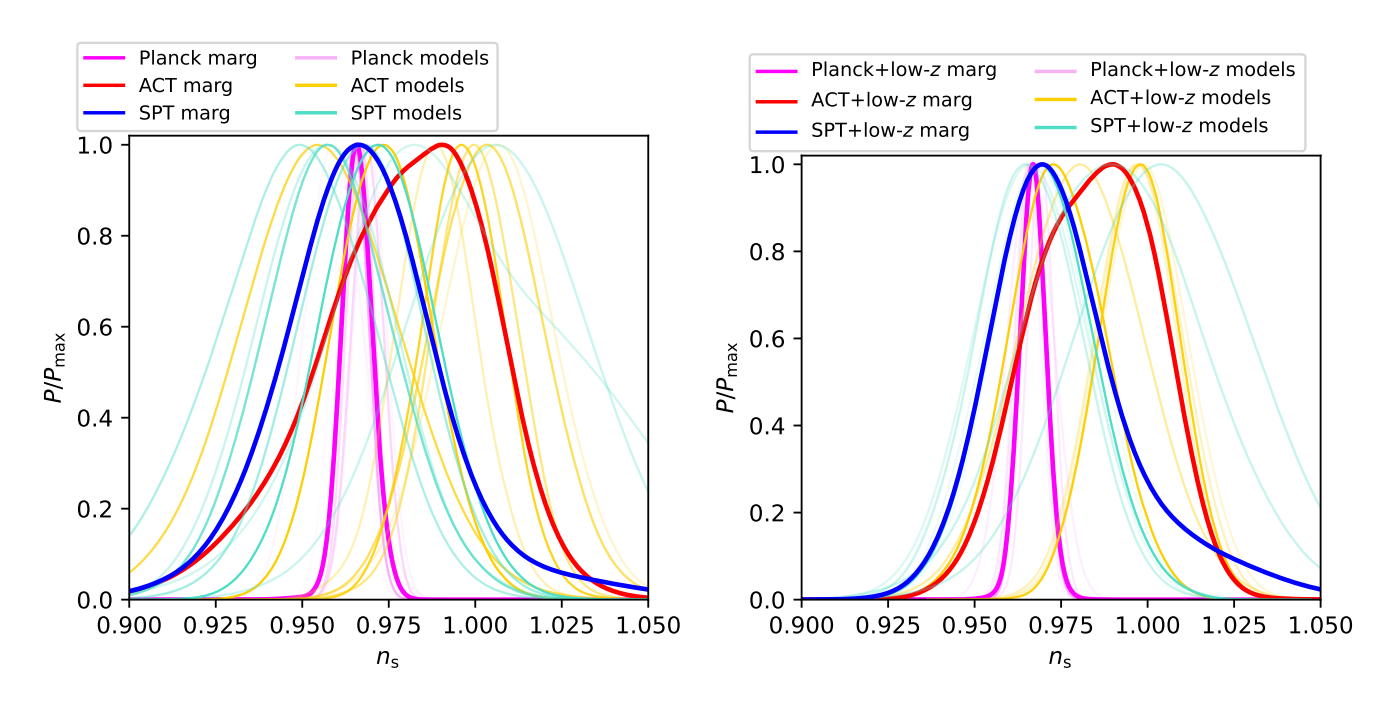


Figure 5: Marginalized 1D posteriors for n_s , considering different datasets. Colors are the same as in Fig. 1.

the results. When varying the fiducial cosmology, i.e. allowing for extensions of the minimal Λ CDM scheme, does not have a very large impact on the mean value and errors of $\theta_{\rm MC}$ except from $N_{\rm eff}$, see Tab. VII. Reference [53] provides analytical expressions for the sound horizon at decoupling and makes straightforward to un-

derstand the large impact of $N_{\rm eff}$ in the mean value and errors of $100\theta_{\rm MC}$. The value of r_s , the sound horizon at decoupling, is directly linked to the amount of radiation in the universe, governed by $N_{\rm eff}$. Therefore, varying this parameter will have an obvious impact on the value of $100\theta_{\rm MC}$.

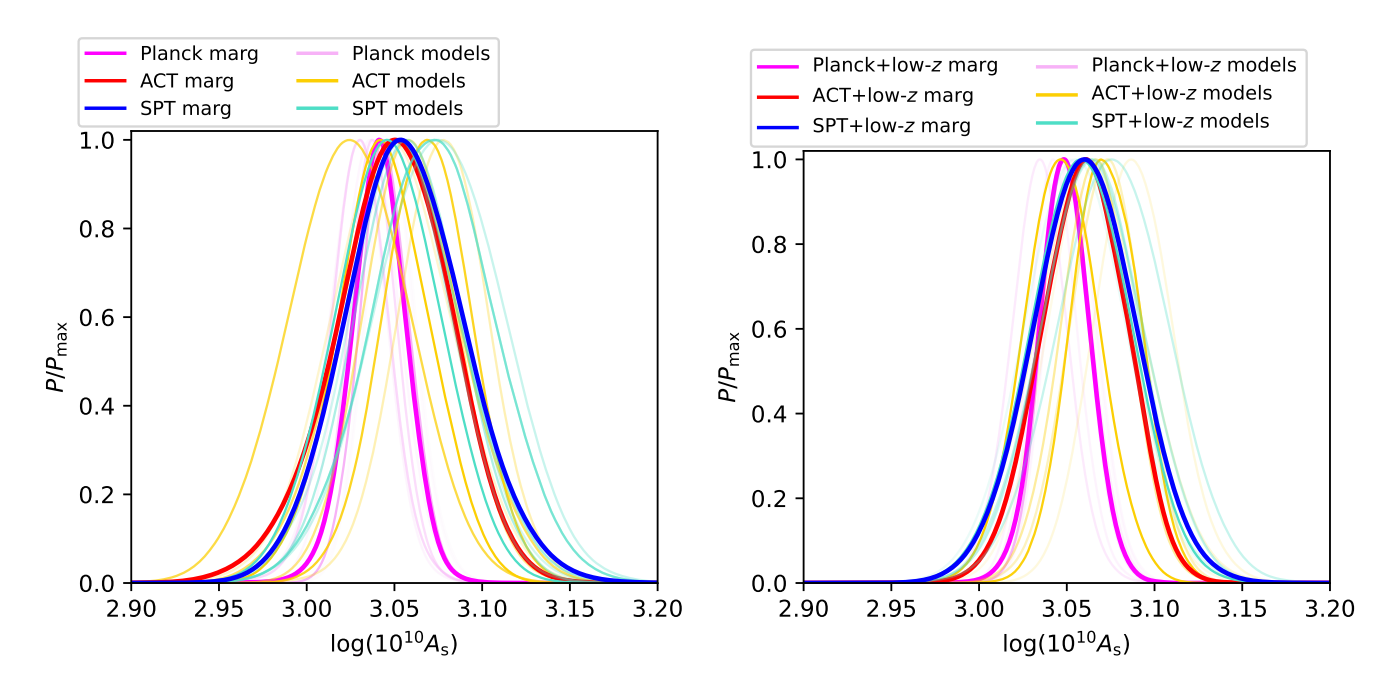


Figure 6: Marginalized 1D posteriors for $\log(10^{10}A_s)$, considering different datasets. Colors are the same as in Fig. 1.

We shall comment next on the marginalized limits of the parameter $\tau_{\rm reio}$, the reionization optical depth. Table $\overline{\text{IV}}$ shows two very important points concerning the extraction of this parameter: firstly, it is Planck that obtains the best accuracy on $\tau_{\rm reio}$ by means of polarization measurements. Indeed, the errors from either the SPT or ACT datasets are a consequence of the Gaussian prior applied while studying high multipole CMB data from these two experiments, which have no sensitivity on $\tau_{\rm reio}$ on their own. Such Gaussian prior is a conservative estimate obtained partially from WMAP and Planck results, see [15], which brings twice as large errors as those obtained from Planck CMB measurements. Secondly, notice that low redshift measurements do not basically change the errors on $\tau_{\rm reio}$ for Planck, due to their lack of sensitivity to the physical effects induced by this parameter. From what regards the different fiducial cosmologies considered here, the largest impact, as expected, is when the phenomenological parameter A_{lens} is allowed to freely vary, see Tab. X. Indeed, the mean value of $\tau_{\rm reio}$ is smaller than its Λ CDM counterpart when the lensing amplitude is a free parameter in the analysis. Even if the shift in such a mean value is not significant, it is straightforward to understand. If $A_{\rm lens} > 1$, CMB lensing will be stronger. Since $\tau_{\rm reio}$ suppresses all acoustic peaks by a constant factor $\exp(-\tau_{\rm reio})$, while leaving the power on the largest scales unaffected, a smaller value of $\tau_{\rm reio}$, leading to a smaller smearing of the small-scale features in the power spectrum, will be required to compensate for such an effect. Nevertheless, the marginalized constraints on the reionization optical depth are extremely stable and pretty robust.

The next parameter we discuss is the primordial power spectrum scalar spectral index, $n_{\rm s}$. Table IV illustrates the fact that low redshift measurements do not imply a major improvement when combined with Planck CMB measurements. Instead, they improve the accuracy in the extraction of n_s when added to SPT or ACT observations. Figure 5 illustrate the one-dimensional probability distribution for the scalar spectral index parameter for different data sets and fiducial cosmologies. The largest departure takes place when the number of relativistic degrees of freedom, $N_{\rm eff}$, is also a free parameter in the fiducial cosmology, see Tab. VII. The effect is straightforward to understand: values $N_{\rm eff} < 3$ would imply less damping in the CMB high multipole region. This effect can be compensated by a lower value of n_s , that will decrease the slope of the angular power spectrum, lowering the right side with respect to the left side. Conversely values $N_{\rm eff} > 3$ requires the mean value of $n_{\rm s}$ to increase in order to compensate for the larger damping induced by a larger dark radiation component. Nevertheless, the marginalized errors are pretty robust and close to their values within the minimal Λ CDM scenario.

Very similar results to those previously discussed for $\tau_{\rm reio}$ are obtained for the amplitude of the primordial power spectrum $A_{\rm s}$, strongly correlated with $\tau_{\rm reio}$: its most accurate measurements arise from Planck, low redshift data does not improve its determination and the largest impact on its error is when the lensing amplitude is a free parameter (see Tab. X), as $A_{\rm s}$ controls the overall normalization of the CMB power spectrum. The two panels of Figure 6 depict the one-dimensional probability distribution for this parameter for different data sets and

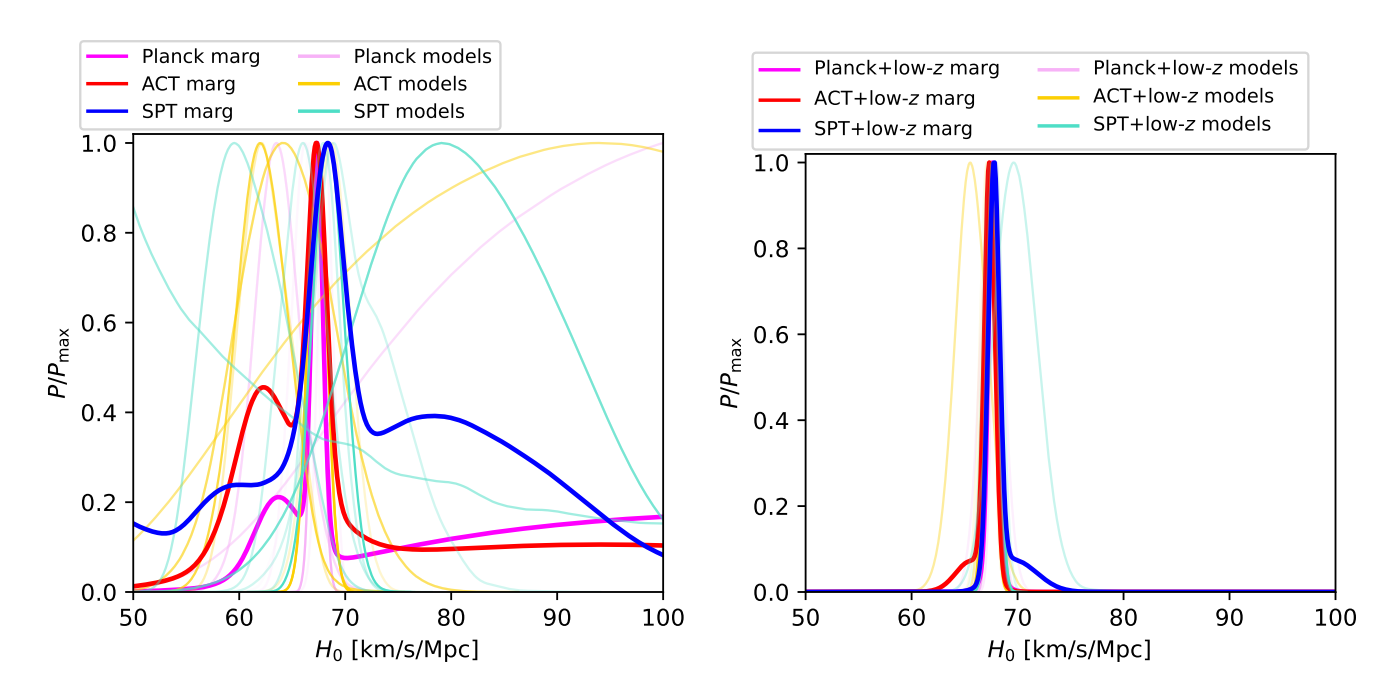


Figure 7: Marginalized 1D posteriors for H_0 [km/s/Mpc], considering different datasets. Colors are the same as in Fig. 1.

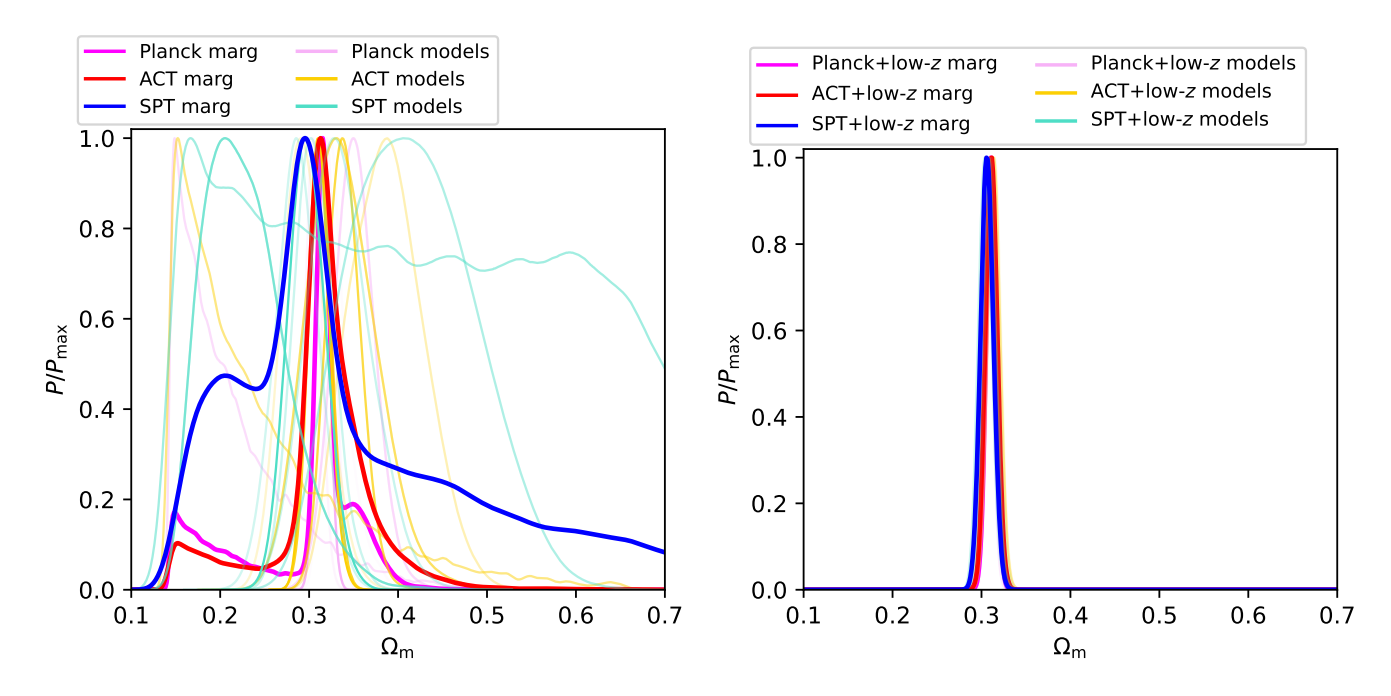


Figure 8: Marginalized 1D posteriors for $\Omega_{\rm m}$, considering different datasets. Colors are the same as in Fig. 1.

fiducial cosmologies.

B. Derived parameters

We have discussed so far the main six Λ CDM parameters. Now we will focus on the derived ones, starting with

the Hubble constant, H_0 . Table IV shows the 95% CL constraints on the Hubble parameter. While the mean value of H_0 is barely shifted, its errors are increased by one to two orders of magnitude when only CMB data are considered, depending on the data set. This case is completely different from what we have observed so far, i.e. low redshift measurements are crucial for restoring the er-

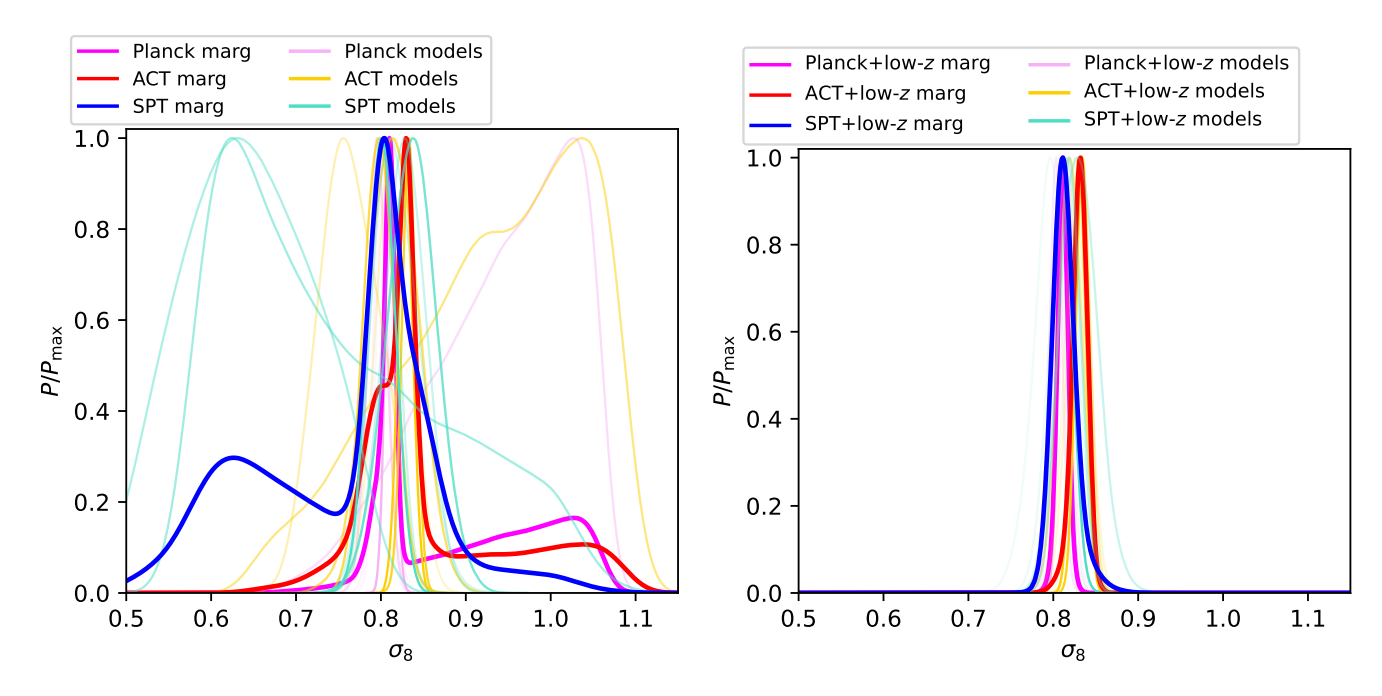


Figure 9: Marginalized 1D posteriors for σ_8 , considering different datasets. Colors are the same as in Fig. 1.

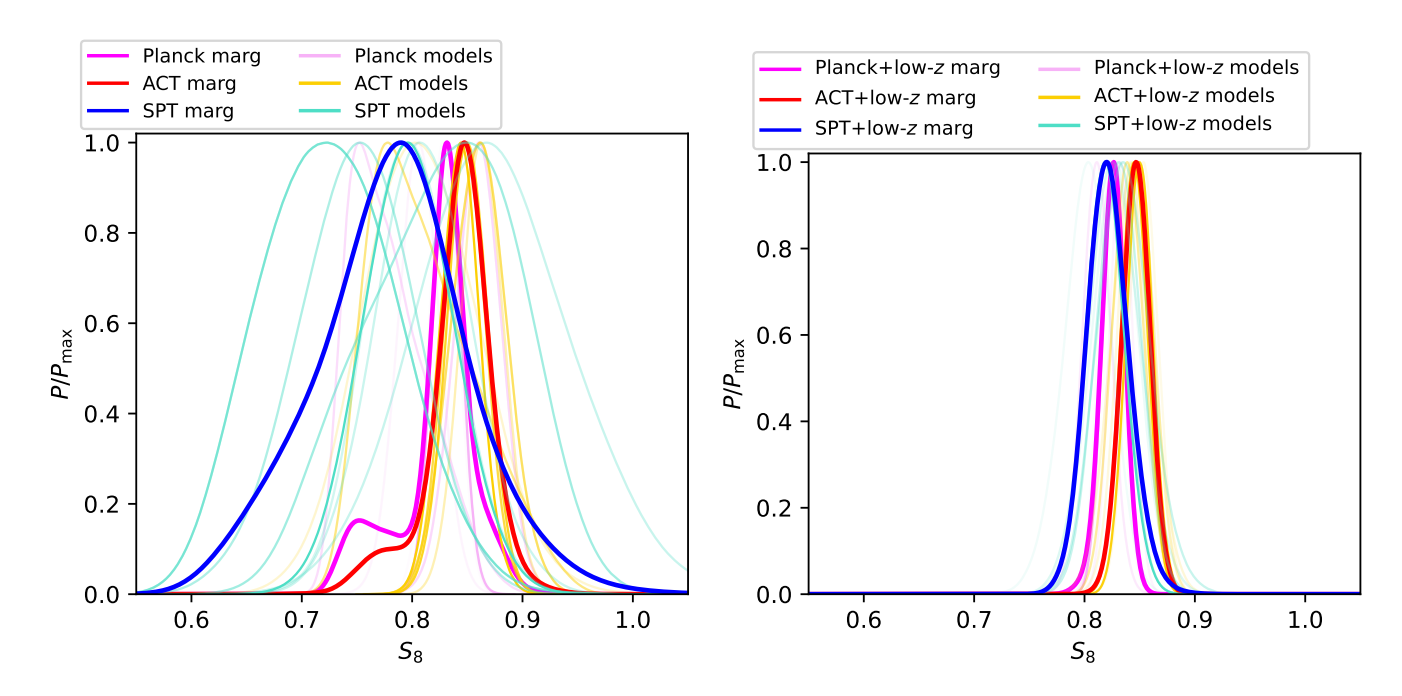


Figure 10: Marginalized 1D posteriors for S_8 , considering different datasets. Colors are the same as in Fig. 1.

rors to their default values within the Λ CDM paradigm, see Tab. V. Once low redshift probes are included in the analyses, the errors on H_0 are decreased by more than one order of magnitude. The very large spread in the errors of the Hubble constant is clearly visible from the left panel of Fig. 7. The right panel shows the dilution of such a spread due to BAO observations, which break many of the degeneracies between H_0 and the cosmo-

logical parameters involved in the extended cosmological scenarios considered here. The largest errors and departures on H_0 are obtained when the dark energy sector is modified. As can be noticed from Tabs. XI and XII, a much larger value of the Hubble constant is obtained when the dark energy equation of state is a freely varying parameter or a function of redshift for the case of Planck and ACT. In addition, the value of the dark energy equa-

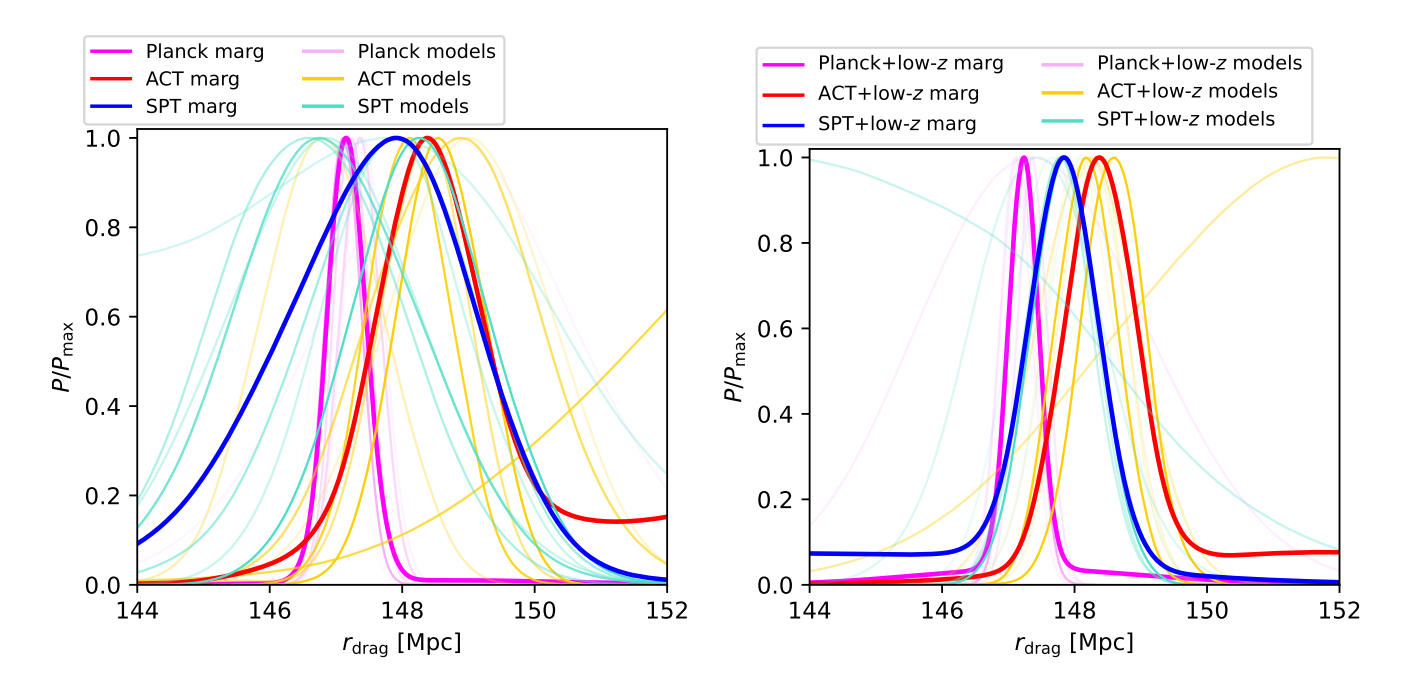


Figure 11: Marginalized 1D posteriors for r_{drag} [Mpc], considering different datasets. Colors are the same as in Fig. 1.

tion of state is preferred to be in the phantom region with a significance of 2σ (in the constant w case). This is a well-known result and indeed it has been proposed as a scenario where to solve the long-standing Hubble constant tension [54]. In the case of SPT, the situation is reversed: a value w>-1 is preferred, and therefore the value of the Hubble parameter is considerably smaller than within the minimal Λ CDM scheme. Nevertheless, also in the SPT case the low redshift data restores mean values and errors of the Hubble constant very close to their Λ CDM counterparts.

The following derived parameter we discuss here is the matter mass energy density parameter, $\Omega_{\rm m}$. As in the previous case, low redshift measurements also affect in a significant way the errors on the marginalized values, see Tab. IV, and their addition reduces the errors by one order of magnitude in some cases. The very large spread in the mean values and errors of $\Omega_{\rm m}$ can be noticed from the left panel of Fig. 8 and the constraining power of lowz data is visible from the right panel of the very same figure. The largest departure in the mean values of the matter density parameter occurs, as in the previous case, when the dark energy sector freedom is enlarged: the reason for that is simple. As we have seen, for the case of Planck and ACT, the Hubble constant can take very large values when w < -1. However, the CMB acoustic peak structure does not allow the quantity $\Omega_{\rm m}h^2$ to be very large, and, consequently, the value of $\Omega_{\rm m}$ is required to be considerably smaller than in the canonical Λ CDM scenario. In the case of SPT the situation is again reversed, and a much larger value of $\Omega_{\rm m}$ is obtained. However, for the three CMB datasets explored here (Planck, ACT

and SPT), when low redshift measurements are included, the value of the dark energy equation of state gets much closer to -1 and the mean values and errors are almost restored to their default values within the Λ CDM picture.

Concerning the remaining derived parameters, i.e. the clustering-related ones σ_8 and S_8 , and $r_{\rm drag}$, low redshift measurements play a major role especially in the case of σ_8 and S_8 . As visible from Figs. 9 and 10, the addition of these measurements dilutes the spread in the mean values and errors of these two clustering parameters, ensuring their stability against different possible fiducial cosmologies. Therefore, it is perfectly valuable to use the marginalized values of these derived parameters when testing exotic cosmological scenarios, due to their stability against different possible fiducial cosmologies.

IV. CONCLUSIONS

Are the Λ CDM model parameters robust? The answer is yes. After analyzing the model-marginalized limits on the standard Λ CDM cosmological parameters $\Omega_{\rm c}h^2$, $\Omega_{\rm b}h^2$, $\theta_{\rm MC}$, $\tau_{\rm reio}$, n_s and A_s as well as on the derived quantities H_0 , $\Omega_{\rm m}$, σ_8 , S_8 and $r_{\rm drag}$ we notice that even if with CMB data only the mean values and errors have large spreads when computed over a number of possible non-minimal fiducial cosmologies, the addition of low redshift measurements restores their values to their canonical Λ CDM ones. Our marginalization procedure includes scenarios with massive neutrinos, extra relativistic species, non-minimal dark energy equation of state

scenarios, non-zero curvature or a varying lensing amplitude parameter. Our results not only demonstrate the stability of the standard cosmological parameters, but also provide a set of marginalized errors and mean values that can be used as an input for cosmological fitting purposes, and they are more reliable and conservative than those obtained within the minimal ΛCDM picture.

ACKNOWLEDGMENTS

EDV is supported by a Royal Society Dorothy Hodgkin Research Fellowship. This article is based upon work from COST Action CA21136 Addressing observational tensions in cosmology with systematics and fundamental physics (CosmoVerse) supported by COST (European Cooperation in Science and Technology). We acknowledge IT Services at The University of Sheffield for the provision of services for High Performance Computing.

S.G. is supported by the European Union's Framework Programme for Research and Innovation Horizon 2020 (2014–2020) under Junior Leader Fellowship LCF/BQ/PI23/11970034 by La Caixa Foundation. This work has been supported by the Spanish MCIN/AEI/10.13039/501100011033 grants PID2020-113644GB-I00 and by the European ITN project HIDDeN (H2020-MSCA-ITN-2019/860881-HIDDeN) and SE project ASYMMETRY (HORIZON-MSCA-2021-SE-01/101086085-ASYMMETRY) and well as by the Generalitat Valenciana grants PROMETEO/2019/083 and CIPROM/2022/69. OM acknowledges the financial support from the MCIU with funding from the European Union NextGenerationEU (PRTR-C17.I01) and Generalitat Valenciana (ASFAE/2022/020).

Appendix A: Tables

In this Appendix we include the tables with all the results for the cosmological parameters within all the models discussed in our work.

Parameter	Planck	Planck+low-z	ACT	ACT+lowz	SPT	SPT+low-z
$\Omega_b h^2$	$0.02238 \pm 0.00014 \big(0.02238^{+0.00028}_{-0.00028} \big)$	$0.02242 \pm 0.00013 (0.02242^{+0.00027}_{-0.00026})$	$0.02163 \pm 0.00030 (0.02163^{+0.00061}_{-0.00057})$	$0.02162 \pm 0.00029 (0.02162^{+0.00058}_{-0.00057})$	$0.02225 \pm 0.00031 (0.02225^{+0.00063}_{-0.00060})$	$0.02223 \pm 0.00031 (0.02223^{+0.00061}_{-0.00060})$
$\Omega_c h^2$	$0.1200 \pm 0.0012 (0.1200^{+0.0024}_{-0.0023})$	$0.11931 \pm 0.00088 (0.1193^{+0.0018}_{-0.0017})$	$0.1194 \pm 0.0021 (0.1194^{+0.0043}_{-0.0042})$	$0.1191 \pm 0.0012 (0.1191^{+0.0023}_{-0.0023})$	$0.1161 \pm 0.0038 (0.1161^{+0.0076}_{-0.0075})$	$0.1178 \pm 0.0013 (0.1178^{+0.0026}_{-0.0026})$
$100\theta_{\mathrm{MC}}$	$1.04091 \pm 0.00031 (1.04091^{+0.00061}_{-0.00061})$	$1.04100 \pm 0.00029 (1.04100^{+0.00056}_{-0.00057})$	$1.04209 \pm 0.00068 (1.0421^{+0.0013}_{-0.0014})$	$1.04213 \pm 0.00061 (1.0421^{+0.0012}_{-0.0012})$	$1.04029 \pm 0.00075 (1.0403^{+0.0015}_{-0.0015})$	$1.04022 \pm 0.00068 (1.0402^{+0.0013}_{-0.0013})$
$ au_{ m reio}$	$0.0543 \pm 0.0076 (0.054^{+0.016}_{-0.015})$	$0.0576 \pm 0.0071 (0.058^{+0.015}_{-0.013})$	$0.069 \pm 0.014 (0.069^{+0.028}_{-0.027})$	$0.071 \pm 0.011 (0.071^{+0.021}_{-0.020})$	$0.059 \pm 0.015 (0.059^{+0.028}_{-0.029})$	$0.063 \pm 0.013 (0.063^{+0.026}_{-0.026})$
$n_{\rm s}$	$0.9651 \pm 0.0041 (0.9651^{+0.0081}_{-0.0079})$	$0.9668 \pm 0.0036 (0.9668^{+0.0071}_{-0.0070})$	$0.996 \pm 0.012 (0.996^{+0.024}_{-0.024})$	$0.998 \pm 0.012 (0.998^{+0.022}_{-0.022})$	$0.972 \pm 0.017 (0.972^{+0.033}_{-0.033})$	$0.969 \pm 0.015 (0.969^{+0.030}_{-0.029})$
$\log(10^{10} A_{\rm s})$	$3.044 \pm 0.015 (3.044^{+0.029}_{-0.028})$	$3.050 \pm 0.014 (3.050^{+0.028}_{-0.027})$	$3.069 \pm 0.025 (3.069^{+0.050}_{-0.050})$	$3.072 \pm 0.019 (3.072^{+0.037}_{-0.038})$	$3.046 \pm 0.030 (3.046^{+0.058}_{-0.060})$	$3.058 \pm 0.029 (3.058^{+0.055}_{-0.057})$
H_0	$67.36 \pm 0.54 (67.4^{+1.1}_{-1.0})$	$67.65 \pm 0.40 (67.65^{+0.78}_{-0.78})$	$67.35 \pm 0.90 (67.4^{+1.8}_{-1.8})$	$67.43 \pm 0.48 (67.43^{+0.98}_{-0.92})$	$68.4 \pm 1.5 (68.4^{+3.1}_{-3.0})$	$67.78 \pm 0.52 (67.8^{+1.0}_{-1.0})$
Ω_{m}	$0.3152 \pm 0.0074 (0.315^{+0.015}_{-0.014})$	$0.3111 \pm 0.0053 (0.311^{+0.011}_{-0.010})$	$0.313 \pm 0.013 (0.313^{+0.026}_{-0.024})$	$0.3110 \pm 0.0065 (0.311^{+0.013}_{-0.013})$	$0.298 \pm 0.021 (0.298^{+0.044}_{-0.040})$	$0.3062 \pm 0.0071 (0.306^{+0.014}_{-0.014})$
σ_8	$0.8111 \pm 0.0061 (0.811^{+0.012}_{-0.012})$	$0.8116 \pm 0.0059 (0.812^{+0.012}_{-0.011})$	$0.8331 \pm 0.0083 (0.833^{+0.016}_{-0.016})$	$0.8343 \pm 0.0078 (0.834^{+0.015}_{-0.015})$	$0.800 \pm 0.016 (0.800^{+0.031}_{-0.032})$	$0.811 \pm 0.012 (0.811^{+0.023}_{-0.023})$
$r_{ m drag}$	$147.11 \pm 0.27 (147.11^{+0.53}_{-0.54})$	$147.22 \pm 0.22 (147.22^{+0.44}_{-0.44})$	$148.11 \pm 0.63 (148.1^{+1.2}_{-1.2})$	$148.18 \pm 0.47 (148.18^{+0.93}_{-0.90})$	$148.3 \pm 1.1 (148.3^{+2.1}_{-2.1})$	$147.86 \pm 0.51 (147.9^{+1.0}_{-1.0})$

Table V: Mean values and 68% (95%) CL constraints on the six Λ CDM parameters as well as on some derived ones $(H_0, \Omega_{\rm m}, \sigma_8 \text{ and } r_{\rm drag})$ within the minimal Λ CDM fiducial cosmology.

Parameter	Planck	Planck+low-z	ACT	ACT+lowz	SPT	SPT+low-z
$\sum m_{\nu} [eV]$	< 0.406	< 0.135	< 0.890	< 0.207	< 2.75	< 0.242
$\Omega_{\rm b}h^2$	$0.02231 \pm 0.00016 (0.02231^{+0.00031}_{-0.00031})$	$0.02243 \pm 0.00013 (0.02243^{+0.00026}_{-0.00026})$	$0.02147 \pm 0.00031 (0.02147^{+0.00059}_{-0.00060})$	$0.02163 \pm 0.00029 (0.02163^{+0.00058}_{-0.00056})$	$0.02218 \pm 0.00032 \big(0.02218^{+0.00062}_{-0.00061} \big)$	$0.02224 \pm 0.00031 (0.02224^{+0.00061}_{-0.00061})$
$\Omega_c h^2$	$0.1206 \pm 0.0013 (0.1206^{+0.0026}_{-0.0025})$	$0.11918 \pm 0.00089 (0.1192^{+0.0017}_{-0.0017})$	$0.1236 \pm 0.0028 (0.1236^{+0.0054}_{-0.0054})$	$0.1185 \pm 0.0012 (0.1185^{+0.0024}_{-0.0025})$	$0.1161^{+0.0056}_{-0.0050} (0.116^{+0.011}_{-0.011})$	$0.1166 \pm 0.0016 (0.1166^{+0.0030}_{-0.0033})$
$100\theta_{\mathrm{MC}}$	$1.04080 \pm 0.00032 (1.04080^{+0.00063}_{-0.00061})$	$1.04101 \pm 0.00029 (1.04101^{+0.00055}_{-0.00056})$	$1.04159 \pm 0.00068 (1.0416^{+0.0013}_{-0.0013})$	$1.04222 \pm 0.00062 (1.0422^{+0.0012}_{-0.0012})$	$1.03984 \pm 0.00075 (1.0398^{+0.0015}_{-0.0015})$	$1.04032 \pm 0.00069 (1.0403^{+0.0013}_{-0.0013})$
$\tau_{\rm reio}$	$0.0553 \pm 0.0075 (0.055^{+0.016}_{-0.014})$	$0.0589 \pm 0.0074 (0.059^{+0.015}_{-0.014})$	$0.070 \pm 0.014 (0.070^{+0.028}_{-0.028})$	$0.078 \pm 0.012 (0.078^{+0.025}_{-0.023})$	$0.061 \pm 0.014 (0.061^{+0.029}_{-0.028})$	$0.067 \pm 0.014 (0.067^{+0.026}_{-0.026})$
n_{s}	$0.9630 \pm 0.0046 (0.9630^{+0.0087}_{-0.0094})$	$0.9671 \pm 0.0036 (0.9671^{+0.0070}_{-0.0071})$	$0.989 \pm 0.012 (0.989^{+0.024}_{-0.024})$	$0.997 \pm 0.012 (0.997^{+0.023}_{-0.023})$	$0.947 \pm 0.023 (0.947^{+0.048}_{-0.050})$	$0.971 \pm 0.015 (0.971^{+0.030}_{-0.029})$
$\log(10^{10}A_{\rm s})$	$3.048 \pm 0.015 (3.048^{+0.030}_{-0.028})$	$3.053 \pm 0.015 (3.053^{+0.029}_{-0.028})$	$3.078 \pm 0.026 (3.078^{+0.050}_{-0.050})$	$3.088 \pm 0.023 (3.088^{+0.046}_{-0.043})$	$3.058 \pm 0.030 (3.058^{+0.059}_{-0.058})$	$3.065 \pm 0.029 (3.065^{+0.057}_{-0.056})$
H_0	$66.1^{+1.4}_{-1.2} (66.1^{+2.5}_{-2.8})$	$67.47 \pm 0.43 (67.47^{+0.83}_{-0.87})$	$62.4 \pm 2.3 (62.4^{+4.6}_{-4.4})$	$67.16 \pm 0.53 (67.2^{+1.0}_{-1.1})$	$60.8 \pm 3.6 (61^{+8}_{-7})$	$67.59 \pm 0.54 (67.6^{+1.1}_{-1.1})$
Ω_{m}	$0.332^{+0.016}_{-0.020} (0.332^{+0.040}_{-0.035})$	$0.3132 \pm 0.0057 (0.313^{+0.011}_{-0.011})$	$0.388 \pm 0.041 (0.388^{+0.087}_{-0.085})$	$0.3136 \pm 0.0069 (0.314^{+0.014}_{-0.013})$	$0.416 \pm 0.068 (0.42^{+0.15}_{-0.14})$	$0.3071 \pm 0.0072 (0.307^{+0.014}_{-0.014})$
σ_8	$0.788^{+0.026}_{-0.020} (0.788^{+0.046}_{-0.052})$	$0.8058 \pm 0.0079 (0.806^{+0.017}_{-0.017})$	$0.762 \pm 0.034 (0.762^{+0.065}_{-0.065})$	$0.824 \pm 0.011 (0.824^{+0.024}_{-0.025})$	$0.644 \pm 0.076 (0.64^{+0.14}_{-0.14})$	$0.793^{+0.021}_{-0.018} (0.793^{+0.038}_{-0.040})$
$r_{ m drag}$	$146.96 \pm 0.30 (146.96^{+0.57}_{-0.61})$	$147.24 \pm 0.22 (147.24^{+0.44}_{-0.43})$	$146.79 \pm 0.90 (146.8^{+1.7}_{-1.7})$	$148.32 \pm 0.47 (148.32^{+0.93}_{-0.93})$	$146.6 \pm 1.4 (146.6^{+2.7}_{-2.7})$	$148.12 \pm 0.56 (148.1^{+1.1}_{-1.1})$

Table VI: Mean values and 68% (95%) CL constraints on the six Λ CDM parameters as well as on some derived ones (H_0 , $\Omega_{\rm m}$, σ_8 and $r_{\rm drag}$) within a fiducial cosmology with massive neutrinos. The 95% CL limits on the total neutrino mass are also presented, for the sake of completeness.

Parameter	Planck	Planck+low-z	ACT	$\mathbf{ACT} + \mathbf{lowz}$	SPT	$\mathbf{SPT} + \mathbf{low-z}$
$N_{\rm eff}$	2.89 ± 0.19 $(2.89^{+0.38}_{-0.36})$	$3.03 \pm 0.17 (3.03^{+0.33}_{-0.33})$	$2.31 \pm 0.34 (2.31^{+0.68}_{-0.65})$	2.72 ± 0.27 $(2.72^{+0.53}_{-0.51})$	$3.45^{+0.54}_{-0.63} (3.5^{+1.2}_{-1.1})$	$3.46 \pm 0.38 (3.46^{+0.84}_{-0.80})$
$\Omega_{\rm b}h^2$	$0.02224 \pm 0.00022 \big(0.02224 ^{+0.00043}_{-0.00042} \big)$	$0.02242 \pm 0.00017 (0.02242^{+0.00034}_{-0.00034})$	$0.02096 \pm 0.00044 (0.02096^{+0.00084}_{-0.00087})$	$0.02135 \pm 0.00036 (0.02135^{+0.00070}_{-0.00071})$	$0.02249 \pm 0.00046 (0.02249^{+0.00099}_{-0.00096})$	$0.02248 \pm 0.00038 (0.02248^{+0.00075}_{-0.00073})$
$\Omega_c h^2$	$0.1178 \pm 0.0029 (0.1178^{+0.0058}_{-0.0055})$	$0.1191 \pm 0.0029 (0.1191^{+0.0057}_{-0.0056})$	$0.1094 \pm 0.0050 (0.109^{+0.010}_{-0.0095})$	$0.1135 \pm 0.0047 (0.1135^{+0.0093}_{-0.0091})$	$0.1216^{+0.0084}_{-0.0094} (0.122^{+0.018}_{-0.017})$	$0.1253 \pm 0.0072 (0.125^{+0.016}_{-0.015})$
$100\theta_{\mathrm{MC}}$	$1.04117 \pm 0.00044 (1.04117^{+0.00086}_{-0.00085})$	$1.04104 \pm 0.00043 (1.04104^{+0.00085}_{-0.00083})$	$1.04321 \pm 0.00089 (1.0432^{+0.0018}_{-0.0017})$	$1.04275 \pm 0.00083 (1.0427^{+0.0016}_{-0.0016})$	$1.03992 \pm 0.00092 (1.0399^{+0.0018}_{-0.0018})$	$1.03963 \pm 0.00086 (1.0396^{+0.0017}_{-0.0017})$
$\tau_{ m reio}$	$0.0533 \pm 0.0074 (0.053^{+0.015}_{-0.014})$	$0.0574 \pm 0.0072 (0.057^{+0.015}_{-0.014})$	$0.060 \pm 0.015 (0.060^{+0.029}_{-0.029})$	$0.074 \pm 0.011 (0.074^{+0.021}_{-0.022})$	$0.061 \pm 0.015 (0.061^{+0.029}_{-0.029})$	0.060 ± 0.013 $(0.060^{+0.026}_{-0.026})$
$n_{\rm s}$	$0.9590 \pm 0.0084 (0.959^{+0.017}_{-0.016})$	$0.9662 \pm 0.0066 (0.966^{+0.013}_{-0.013})$	$0.955 \pm 0.023 (0.955^{+0.045}_{-0.046})$	$0.981 \pm 0.018 (0.981^{+0.036}_{-0.035})$	$0.997 \pm 0.037 (0.997^{+0.080}_{-0.076})$	$0.991 \pm 0.025 (0.991^{+0.051}_{-0.048})$
$\log(10^{10}A_{\rm s})$	$3.036 \pm 0.017 (3.036^{+0.034}_{-0.034})$	$3.049 \pm 0.016 (3.049^{+0.031}_{-0.030})$	$3.024 \pm 0.034 (3.024^{+0.065}_{-0.068})$	$3.066 \pm 0.020 (3.066^{+0.038}_{-0.040})$	$3.056 \pm 0.032 (3.056^{+0.063}_{-0.065})$	$3.063 \pm 0.028 (3.063^{+0.054}_{-0.056})$
H_0	$66.3 \pm 1.4 (66.3^{+2.8}_{-2.6})$	$67.6 \pm 1.1 (67.6^{+2.1}_{-2.1})$	$62.2 \pm 2.5 (62.2^{+5.0}_{-4.9})$	$65.7 \pm 1.5 (65.7^{+3.1}_{-3.0})$	$71.3^{+4.1}_{-4.7} (71^{+9}_{-8})$	$69.9 \pm 2.0 (69.9^{+4.3}_{-4.2})$
Ω_{m}	$0.3200 \pm 0.0096 (0.320^{+0.019}_{-0.019})$	$0.3113 \pm 0.0059 (0.311^{+0.012}_{-0.011})$	$0.339 \pm 0.019 (0.339^{+0.042}_{-0.040})$	$0.3143 \pm 0.0071 (0.314^{+0.014}_{-0.014})$	$0.287 \pm 0.025 (0.287^{+0.050}_{-0.049})$	$0.3038 \pm 0.0074 (0.304^{+0.015}_{-0.014})$
σ_8	$0.8048 \pm 0.0097 (0.805^{+0.019}_{-0.019})$	$0.8108 \pm 0.0094 (0.811^{+0.019}_{-0.018})$	$0.798 \pm 0.018 (0.798^{+0.036}_{-0.035})$	$0.820 \pm 0.014 (0.820^{+0.028}_{-0.027})$	$0.819 \pm 0.028 (0.819^{+0.061}_{-0.058})$	$0.831 \pm 0.022 (0.831^{+0.048}_{-0.046})$
$r_{ m drag}$	$148.7 \pm 1.9 (148.7^{+3.7}_{-3.7})$	$147.4 \pm 1.7 (147.4^{+3.4}_{-3.3})$	$155.9 \pm 3.8 (155.9^{+7.8}_{-7.3})$	$151.8 \pm 3.1 (151.8^{+6.1}_{-5.8})$	$144.8 \pm 4.8 (144.8^{+9.9}_{-10})$	$143.8 \pm 3.8 (143.8^{+7.1}_{-7.5})$

Table VII: Mean values and 68% (95%) CL constraints on the six Λ CDM parameters as well as on some derived ones (H_0 , $\Omega_{\rm m}$, σ_8 and $r_{\rm drag}$) within a fiducial cosmology with $N_{\rm eff}$ a free parameter. The mean values and errors on the relativistic degrees of freedom at decoupling also presented, for the sake of completeness.

Parameter	Planck	Planck+low-z	ACT	ACT+lowz	SPT	$\mathbf{SPT} + \mathbf{low-z}$
α_s	$-0.0049 \pm 0.0067 \left(-0.005^{+0.013}_{-0.013}\right)$	$-0.0046 \pm 0.0068 (-0.005^{+0.013}_{-0.013})$	$0.066 \pm 0.023 (0.066^{+0.045}_{-0.046})$	$0.065 \pm 0.024 (0.065^{+0.046}_{-0.046})$	$-0.071 \pm 0.041 (-0.071^{+0.079}_{-0.081})$	$-0.070 \pm 0.040 (-0.070^{+0.079}_{-0.079})$
$\Omega_{\rm b}h^2$	$0.02241 \pm 0.00015 (0.02241^{+0.00030}_{-0.00029})$	$0.02246 \pm 0.00014 (0.02246^{+0.00027}_{-0.00028})$	$0.02134 \pm 0.00032 (0.02134^{+0.00061}_{-0.00062})$	$0.02133 \pm 0.00032 (0.02133^{+0.00063}_{-0.00061})$	$0.02229 \pm 0.00031 (0.02229^{+0.00062}_{-0.00061})$	$0.02228 \pm 0.00031 (0.02228^{+0.00062}_{-0.00062})$
$\Omega_{\rm c} h^2$	$0.1200 \pm 0.0012 (0.1200^{+0.0024}_{-0.0023})$	$0.11935 \pm 0.00087 (0.1194^{+0.0017}_{-0.0017})$	$0.1188 \pm 0.0021 (0.1188^{+0.0043}_{-0.0041})$	$0.1189 \pm 0.0012 (0.1189^{+0.0023}_{-0.0023})$	$0.1175 \pm 0.0040 (0.1175^{+0.0081}_{-0.0078})$	$0.1179 \pm 0.0013 (0.1179^{+0.0026}_{-0.0026})$
$100\theta_{\mathrm{MC}}$	$1.04090 \pm 0.00031 (1.04090^{+0.00060}_{-0.00061})$	$1.04100 \pm 0.00029 (1.04100^{+0.00057}_{-0.00055})$	$1.04225 \pm 0.00067 (1.0422^{+0.0013}_{-0.0013})$	$1.04222 \pm 0.00063 (1.0422^{+0.0013}_{-0.0012})$	$1.04010 \pm 0.00077 (1.0401^{+0.0015}_{-0.0015})$	$1.04014 \pm 0.00068 (1.0401^{+0.0013}_{-0.0014})$
$ au_{ m reio}$	$0.0553 \pm 0.0077 (0.055^{+0.016}_{-0.015})$	$0.0586 \pm 0.0074 (0.059^{+0.015}_{-0.014})$	$0.059 \pm 0.015 (0.059^{+0.029}_{-0.028})$	$0.061 \pm 0.011 (0.061^{+0.022}_{-0.022})$	$0.062 \pm 0.015 (0.062^{+0.029}_{-0.029})$	$0.068 \pm 0.014 (0.068^{+0.027}_{-0.027})$
$n_{\rm s}$	$0.9641 \pm 0.0043 (0.9641^{+0.0086}_{-0.0085})$	$0.9659 \pm 0.0038 (0.9659^{+0.0074}_{-0.0076})$	$0.973 \pm 0.014 (0.973^{+0.028}_{-0.027})$	$0.974 \pm 0.014 (0.974^{+0.028}_{-0.027})$	$1.006 \pm 0.026 (1.006^{+0.051}_{-0.051})$	$1.005 \pm 0.026 (1.005^{+0.050}_{-0.050})$
$\log(10^{10}A_s)$	$3.048 \pm 0.015 \left(3.048^{+0.031}_{-0.029}\right)$	$3.053 \pm 0.015 (3.053^{+0.030}_{-0.028})$	$3.044 \pm 0.027 (3.044^{+0.052}_{-0.053})$	$3.047 \pm 0.022 (3.047^{+0.042}_{-0.042})$	$3.052 \pm 0.031 (3.052^{+0.059}_{-0.060})$	$3.065 \pm 0.029 (3.065^{+0.057}_{-0.056})$
H_0	$67.35 \pm 0.54 (67.4^{+1.1}_{-1.1})$	$67.67 \pm 0.40 (67.67^{+0.77}_{-0.77})$	$67.36 \pm 0.89 (67.4^{+1.7}_{-1.8})$	$67.33 \pm 0.49 (67.33^{+0.96}_{-0.94})$	$67.9 \pm 1.6 (67.9^{+3.2}_{-3.1})$	$67.76 \pm 0.52 (67.8^{+1.0}_{-1.0})$
$\Omega_{\rm m}$	$0.3156 \pm 0.0074 (0.316^{+0.015}_{-0.014})$	$0.3112 \pm 0.0053 (0.311^{+0.010}_{-0.010})$	$0.311 \pm 0.013 (0.311^{+0.026}_{-0.024})$	$0.3108 \pm 0.0065 (0.311^{+0.013}_{-0.012})$	$0.305 \pm 0.023 (0.305^{+0.050}_{-0.048})$	$0.3068 \pm 0.0071 (0.307^{+0.014}_{-0.014})$
σ_8	$0.8112 \pm 0.0060 (0.811^{+0.012}_{-0.012})$	$0.8116 \pm 0.0059 (0.812^{+0.012}_{-0.011})$	$0.8288 \pm 0.0086 (0.829^{+0.017}_{-0.017})$	$0.8302 \pm 0.0080 (0.830^{+0.016}_{-0.016})$	$0.804 \pm 0.017 (0.804^{+0.033}_{-0.034})$	$0.810 \pm 0.012 (0.810^{+0.023}_{-0.023})$
$r_{ m drag}$	$147.05 \pm 0.27 (147.05^{+0.53}_{-0.53})$	$147.18 \pm 0.23 (147.18^{+0.45}_{-0.44})$	$148.58 \pm 0.66 (148.6^{+1.3}_{-1.3})$	$148.58 \pm 0.49 (148.58^{+0.98}_{-0.96})$	$147.9 \pm 1.1 (147.9^{+2.2}_{-2.2})$	$147.77 \pm 0.52 (147.8^{+1.0}_{-1.0})$

Table VIII: Mean values and 68% (95%) CL constraints on the six Λ CDM parameters as well as on some derived ones (H_0 , $\Omega_{\rm m}$, σ_8 and $r_{\rm drag}$) within a fiducial cosmology with a running of the scalar spectral index. The mean values and errors on $\alpha_{\rm s}$ are also presented, for the sake of completeness.

Parameter	Planck	Planck+low-z	ACT	ACT+lowz	SPT	SPT+low-z
Ω_k	$-0.0104 \pm 0.0065 (-0.010^{+0.014}_{-0.014})$	$0.0006 \pm 0.0017 (0.0006^{+0.0033}_{-0.0035})$	$-0.010^{+0.017}_{-0.015} (-0.010^{+0.031}_{-0.033})$	$0.0000 \pm 0.0029 (0.0000^{+0.0057}_{-0.0056})$	$0.020^{+0.015}_{-0.012} (0.020^{+0.027}_{-0.029})$	$0.0018 \pm 0.0034 (0.0018^{+0.0068}_{-0.0065})$
$\Omega_{\rm b}h^2$	$0.02249 \pm 0.00016 (0.02249^{+0.00031}_{-0.00031})$	$0.02240 \pm 0.00015 (0.02240 ^{+0.00029}_{-0.00029})$	$0.02165 \pm 0.00030 (0.02165^{+0.00061}_{-0.00058})$	$0.02162 \pm 0.00029 (0.02162^{+0.00058}_{-0.00057})$	$0.02212 \pm 0.00032 (0.02212^{+0.00063}_{-0.00062})$	$0.02222 \pm 0.00031 (0.02222^{+0.00060}_{-0.00061})$
$\Omega_{\rm c}h^2$	$0.1185 \pm 0.0015 (0.1185 ^{+0.0029}_{-0.0028})$	$0.1196 \pm 0.0013 (0.1196^{+0.0025}_{-0.0025})$	$0.1167 \pm 0.0047 (0.1167^{+0.0092}_{-0.0089})$	$0.1191 \pm 0.0027 (0.1191^{+0.0054}_{-0.0051})$	$0.1220 \pm 0.0056 (0.122^{+0.011}_{-0.011})$	$0.1195 \pm 0.0035 (0.1195^{+0.0070}_{-0.0068})$
$100\theta_{\rm MC}$	$1.04107 \pm 0.00032 (1.04107^{+0.00062}_{-0.00062})$	$1.04095 \pm 0.00031 (1.04095 ^{+0.00062}_{-0.00061})$	$1.04231 \pm 0.00075 (1.0423^{+0.0015}_{-0.0015})$	$1.04213 \pm 0.00069 (1.0421^{+0.0013}_{-0.0014})$	$1.03983 \pm 0.00080 (1.0398^{+0.0016}_{-0.0016})$	$1.04004 \pm 0.00075 (1.0400^{+0.0015}_{-0.0015})$
$\tau_{ m reio}$	$0.0493 \pm 0.0084 (0.049^{+0.016}_{-0.017})$	$0.0568 \pm 0.0071 (0.057^{+0.015}_{-0.013})$	$0.065 \pm 0.015 (0.065^{+0.030}_{-0.029})$	$0.070 \pm 0.012 (0.070^{+0.024}_{-0.024})$	$0.063 \pm 0.015 (0.063^{+0.029}_{-0.029})$	$0.061 \pm 0.014 (0.061^{+0.028}_{-0.027})$
n_{s}	$0.9688 \pm 0.0046 (0.9688^{+0.0089}_{-0.0090})$	$0.9661 \pm 0.0043 (0.9661^{+0.0084}_{-0.0084})$	$1.004 \pm 0.016 (1.004^{+0.032}_{-0.031})$	$0.997 \pm 0.012 (0.997^{+0.024}_{-0.024})$	$0.958 \pm 0.019 (0.958^{+0.038}_{-0.037})$	$0.966 \pm 0.017 (0.966^{+0.033}_{-0.032})$
$\log(10^{10}A_s)$	$3.030 \pm 0.017 (3.030^{+0.034}_{-0.036})$	$3.049 \pm 0.014 (3.049^{+0.028}_{-0.027})$	$3.053 \pm 0.034 (3.053^{+0.067}_{-0.066})$	$3.072 \pm 0.021 (3.072^{+0.040}_{-0.041})$	$3.072 \pm 0.035 (3.072^{+0.069}_{-0.069})$	$3.058 \pm 0.029 (3.058^{+0.057}_{-0.055})$
H_0	$63.6 \pm 2.2 (63.6^{+4.6}_{-4.3})$	$67.82 \pm 0.57 (67.8^{+1.1}_{-1.1})$	$64.5 \pm 4.5 (65^{+9}_{-8})$	$67.44 \pm 0.65 (67.4^{+1.3}_{-1.2})$	81^{+10}_{-9} (81^{+20}_{-20})	$67.98 \pm 0.64 (68.0^{+1.3}_{-1.3})$
$\Omega_{\rm m}$	$0.351 \pm 0.024 (0.351^{+0.048}_{-0.045})$	$0.3103 \pm 0.0056 (0.310^{+0.011}_{-0.011})$	$0.338 \pm 0.040 (0.338^{+0.087}_{-0.083})$	$0.3109 \pm 0.0067 (0.311^{+0.013}_{-0.013})$	$0.229^{+0.047}_{-0.055} (0.229^{+0.11}_{-0.098})$	$0.3081 \pm 0.0079 (0.308^{+0.016}_{-0.015})$
σ_8	$0.795 \pm 0.011 (0.795^{+0.022}_{-0.023})$	$0.8125 \pm 0.0068 (0.813^{+0.013}_{-0.013})$	$0.814 \pm 0.030 (0.814^{+0.057}_{-0.057})$	$0.8340 \pm 0.0094 (0.834^{+0.019}_{-0.019})$	$0.836 \pm 0.030 (0.836^{+0.058}_{-0.059})$	$0.816 \pm 0.016 (0.816^{+0.031}_{-0.031})$
$r_{ m drag}$	$147.36 \pm 0.30 (147.36^{+0.59}_{-0.60})$	$147.16 \pm 0.28 (147.16^{+0.56}_{-0.54})$	$148.8 \pm 1.3 (148.8^{+2.5}_{-2.4})$	$148.19 \pm 0.76 (148.2^{+1.5}_{-1.5})$	$146.9 \pm 1.4 (146.9^{+2.8}_{-2.8})$	$147.42 \pm 0.98 (147.4^{+1.9}_{-1.9})$

Table IX: Mean values and 68% (95%) CL constraints on the six Λ CDM parameters as well as on some derived ones $(H_0, \Omega_{\rm m}, \sigma_8 \text{ and } r_{\rm drag})$ within a fiducial cosmology with a non-zero spatial curveture. The mean values and errors on the curvature parameter $\Omega_{\rm k}$ are also presented, for the sake of completeness.

Parameter	Planck	Planck+low-z	ACT	ACT+lowz	SPT	$\mathbf{SPT} + \mathbf{low-z}$
A_{lens}	$1.071 \pm 0.041 (1.071^{+0.084}_{-0.078})$	$1.061 \pm 0.035 (1.061^{+0.070}_{-0.066})$	$1.081 \pm 0.092 (1.08^{+0.20}_{-0.19})$	$1.020 \pm 0.045 (1.020^{+0.092}_{-0.085})$	$0.85 \pm 0.10 (0.85^{+0.22}_{-0.21})$	$0.885 \pm 0.077 (0.88^{+0.16}_{-0.15})$
$\Omega_b h^2$	$0.02251 \pm 0.00017 (0.02251^{+0.00033}_{-0.00032})$	$0.02250 \pm 0.00014 (0.02250 ^{+0.00027}_{-0.00027})$	$0.02164 \pm 0.00030 (0.02164^{+0.00059}_{-0.00056})$	$0.02161 \pm 0.00029 (0.02161^{+0.00057}_{-0.00056})$	$0.02213 \pm 0.00032 \big(0.02213 ^{+0.00064}_{-0.00063} \big)$	$0.02218 \pm 0.00031 (0.02218^{+0.00063}_{-0.00060})$
$\Omega_c h^2$	$0.1182 \pm 0.0015 (0.1182^{+0.0030}_{-0.0030})$	$0.11851 \pm 0.00097 (0.1185^{+0.0019}_{-0.0019})$	$0.1160 \pm 0.0045 (0.1160^{+0.0089}_{-0.0084})$	$0.1188 \pm 0.0013 (0.1188^{+0.0026}_{-0.0025})$	$0.1222 \pm 0.0059 (0.122^{+0.012}_{-0.011})$	$0.1182 \pm 0.0014 \big(0.1182^{+0.0027}_{-0.0027}\big)$
$100\theta_{\rm MC}$	$1.04109 \pm 0.00032 (1.04109^{+0.00063}_{-0.00064})$	$1.04108 \pm 0.00029 (1.04108^{+0.00057}_{-0.00057})$	$1.04237 \pm 0.00074 (1.0424^{+0.0014}_{-0.0014})$	$1.04212 \pm 0.00062 (1.0421^{+0.0012}_{-0.0012})$	$1.03983 \pm 0.00081 (1.0398^{+0.0016}_{-0.0016})$	$1.04019 \pm 0.00067 (1.0402^{+0.0013}_{-0.0013})$
$ au_{ m reio}$	$0.0491 \pm 0.0084 (0.049^{+0.018}_{-0.019})$	$0.0513 \pm 0.0080 (0.051^{+0.016}_{-0.016})$	$0.064 \pm 0.015 (0.064^{+0.029}_{-0.030})$	$0.067 \pm 0.014 (0.067^{+0.027}_{-0.028})$	$0.065 \pm 0.015 (0.065^{+0.029}_{-0.029})$	$0.070 \pm 0.014 (0.070^{+0.027}_{-0.028})$
n_{s}	$0.9696 \pm 0.0048 (0.9696^{+0.0096}_{-0.0094})$	$0.9690 \pm 0.0038 (0.9690^{+0.0075}_{-0.0074})$	$1.006 \pm 0.016 (1.006^{+0.032}_{-0.032})$	$0.999 \pm 0.013 (0.999^{+0.025}_{-0.024})$	$0.957 \pm 0.020 (0.957^{+0.039}_{-0.038})$	$0.966 \pm 0.015 (0.966^{+0.030}_{-0.030})$
$\log(10^{10}A_{\rm s})$	$3.028 \pm 0.018 (3.028^{+0.038}_{-0.039})$	$3.034 \pm 0.017 (3.034^{+0.033}_{-0.034})$	$3.048 \pm 0.034 (3.048^{+0.066}_{-0.066})$	$3.063 \pm 0.031 (3.063^{+0.060}_{-0.060})$	$3.076 \pm 0.036 (3.076^{+0.070}_{-0.071})$	$3.076 \pm 0.031 (3.076^{+0.062}_{-0.061})$
H_0	$68.14 \pm 0.70 (68.1^{+1.4}_{-1.4})$	$68.03 \pm 0.44 (68.03^{+0.88}_{-0.85})$	$68.7 \pm 1.8 (68.7^{+3.6}_{-3.5})$	$67.54 \pm 0.51 (67.5^{+1.0}_{-1.0})$	$66.1 \pm 2.3 (66.1^{+4.6}_{-4.3})$	$67.58 \pm 0.53 (67.6^{+1.1}_{-1.0})$
Ω_{m}	$0.3047 \pm 0.0092 (0.305^{+0.018}_{-0.018})$	$0.3062 \pm 0.0058 (0.306^{+0.011}_{-0.011})$	$0.294 \pm 0.025 (0.294^{+0.054}_{-0.052})$	$0.3094 \pm 0.0071 (0.309^{+0.014}_{-0.014})$	$0.334 \pm 0.036 (0.334^{+0.079}_{-0.076})$	$0.3089 \pm 0.0074 (0.309^{+0.015}_{-0.014})$
σ_8	$0.7998 \pm 0.0088 (0.800^{+0.017}_{-0.018})$	$0.8029 \pm 0.0076 (0.803^{+0.015}_{-0.015})$	$0.816 \pm 0.021 (0.816^{+0.041}_{-0.041})$	0.830 ± 0.013 $(0.830^{+0.025}_{-0.025})$	$0.828 \pm 0.025 (0.828^{+0.048}_{-0.050})$	$0.819 \pm 0.013 (0.819^{+0.026}_{-0.026})$
$r_{ m drag}$	$147.41 \pm 0.31 \big(147.41^{+0.62}_{-0.61}\big)$	$147.36 \pm 0.23 (147.36^{+0.46}_{-0.47})$	$149.0 \pm 1.2 (149.0^{+2.3}_{-2.4})$	$148.27 \pm 0.51 (148.3^{+1.0}_{-0.97})$	$146.8 \pm 1.5 (146.8^{+3.0}_{-2.9})$	$147.80 \pm 0.52 (147.8^{+1.0}_{-1.0})$

Table X: Mean values and 68% (95%) CL constraints on the six Λ CDM parameters as well as on some derived ones (H_0 , $\Omega_{\rm m}$, σ_8 and $r_{\rm drag}$) within a fiducial cosmology with a varying lensing amplitude. The mean values and errors on $A_{\rm lens}$ are also presented, for the sake of completeness.

Parameter	Planck	Planck+low-z	ACT	$\mathbf{ACT} + \mathbf{lowz}$	SPT	SPT+low-z
w_0	$-1.55^{+0.26}_{-0.31} \left(-1.55^{+0.57}_{-0.54}\right)$	$-0.995 \pm 0.024 (-0.995^{+0.047}_{-0.048})$	$-1.43^{+0.35}_{-0.42} \left(-1.43^{+0.77}_{-0.72}\right)$	$-0.975 \pm 0.027 \left(-0.975^{+0.052}_{-0.055}\right)$	$-0.76^{+0.58}_{-0.43} (-0.76^{+0.94}_{-1.0})$	$-0.966 \pm 0.029 (-0.966^{+0.056}_{-0.057})$
$\Omega_{\rm b}h^2$	$0.02243 \pm 0.00015 (0.02243^{+0.00029}_{-0.00029})$	$0.02244 \pm 0.00013 (0.02244^{+0.00027}_{-0.00026})$	$0.02160 \pm 0.00030 (0.02160^{+0.00058}_{-0.00058})$	$0.02164 \pm 0.00030 (0.02164^{+0.00060}_{-0.00058})$	$0.02219 \pm 0.00032 \big(0.02219^{+0.00063}_{-0.00062} \big)$	$0.02225 \pm 0.00031 (0.02225^{+0.00062}_{-0.00061})$
$\Omega_c h^2$	$0.1193 \pm 0.0012 \big(0.1193 ^{+0.0024}_{-0.0024} \big)$	$0.11921 \pm 0.00098 (0.1192^{+0.0019}_{-0.0019})$	$0.1187 \pm 0.0023 (0.1187^{+0.0050}_{-0.0049})$	$0.1183 \pm 0.0015 (0.1183^{+0.0029}_{-0.0029})$	$0.1194^{+0.0055}_{-0.0062} \left(0.119^{+0.012}_{-0.011}\right)$	$0.1164 \pm 0.0018 (0.1164^{+0.0035}_{-0.0035})$
$100\theta_{\mathrm{MC}}$	$1.04098 \pm 0.00031 (1.04098^{+0.00060}_{-0.00060})$	$1.04102 \pm 0.00029 (1.04102^{+0.00057}_{-0.00058})$	$1.04213 \pm 0.00066 (1.0421^{+0.0013}_{-0.0013})$	$1.04222 \pm 0.00064 (1.0422^{+0.0012}_{-0.0012})$	$1.04004 \pm 0.00080 (1.0400^{+0.0015}_{-0.0016})$	$1.04033 \pm 0.00069 (1.0403^{+0.0013}_{-0.0014})$
$\tau_{\rm reio}$	$0.0524 \pm 0.0074 (0.052^{+0.015}_{-0.015})$	$0.0579 \pm 0.0074 (0.058^{+0.015}_{-0.014})$	$0.066 \pm 0.014 (0.066^{+0.027}_{-0.027})$	$0.076 \pm 0.012 (0.076^{+0.025}_{-0.024})$	$0.061 \pm 0.015 (0.061^{+0.029}_{-0.029})$	$0.067 \pm 0.014 (0.067^{+0.027}_{-0.027})$
n_{s}	$0.9666 \pm 0.0042 (0.9666^{+0.0082}_{-0.0081})$	$0.9671 \pm 0.0038 (0.9671^{+0.0074}_{-0.0073})$	$0.9997 \pm 0.012 (0.9997^{+0.024}_{-0.024})$	0.998 ± 0.012 $(0.998^{+0.023}_{-0.023})$	$0.964 \pm 0.019 (0.964^{+0.036}_{-0.039})$	$0.972 \pm 0.015 (0.972^{+0.030}_{-0.030})$
$\log(10^{10}A_{\rm s})$	$3.038 \pm 0.014 (3.038^{+0.029}_{-0.028})$	$3.051 \pm 0.014 (3.051^{+0.029}_{-0.027})$	$3.060 \pm 0.026 (3.060^{+0.051}_{-0.051})$	$3.082 \pm 0.023 (3.082^{+0.045}_{-0.044})$	$3.060 \pm 0.035 (3.060^{+0.072}_{-0.066})$	$3.063 \pm 0.029 (3.063^{+0.057}_{-0.057})$
H_0	> 81.8 (> 69.7)	$67.54 \pm 0.65 (67.5^{+1.3}_{-1.3})$	> 76.4 (> 60.7)	$67.02 \pm 0.68 (67.0^{+1.4}_{-1.3})$	62^{+10}_{-20} (62^{+30}_{-30})	$67.27 \pm 0.67 (67.3^{+1.3}_{-1.3})$
Ω_{m}	$0.200^{+0.043}_{-0.061} (0.20^{+0.11}_{-0.10})$	$0.3120 \pm 0.0065 (0.312^{+0.013}_{-0.012})$	$0.225^{+0.066}_{-0.10} (0.23^{+0.17}_{-0.17})$	$0.3131 \pm 0.0071 (0.313^{+0.015}_{-0.013})$	$0.43 \pm 0.17 (0.43^{+0.35}_{-0.36})$	$0.3079 \pm 0.0072 (0.308^{+0.014}_{-0.014})$
σ_8	$0.961^{+0.085}_{-0.072} (0.96^{+0.15}_{-0.16})$	$0.8099 \pm 0.0090 (0.810^{+0.018}_{-0.018})$	$0.95^{+0.12}_{-0.10} (0.95^{+0.20}_{-0.22})$	$0.828 \pm 0.011 (0.828^{+0.021}_{-0.021})$	$0.74^{+0.12}_{-0.16} (0.74^{+0.28}_{-0.26})$	$0.798 \pm 0.016 (0.798^{+0.031}_{-0.031})$
$r_{ m drag}$	$147.22 \pm 0.27 (147.22^{+0.52}_{-0.52})$	$147.24 \pm 0.24 \big(147.24^{+0.47}_{-0.46}\big)$	$148.32 \pm 0.68 (148.3^{+1.3}_{-1.4})$	$148.38 \pm 0.51 (148.38^{+0.98}_{-1.0})$	$147.5 \pm 1.4 (147.5^{+3.0}_{-3.1})$	$148.21 \pm 0.59 (148.2^{+1.2}_{-1.1})$

Table XI: Mean values and 68% (95%) CL constraints on the six Λ CDM parameters as well as on some derived ones $(H_0, \Omega_{\rm m}, \sigma_8 \text{ and } r_{\rm drag})$ within a fiducial cosmology with a varying dark energy equation of state. The mean values and errors on w are also presented, for the sake of completeness.

Parameter	Planck	Planck+low-z	ACT	$\mathbf{ACT} + \mathbf{lowz}$	SPT	SPT+low-z
$\overline{w_0}$	$-1.24 \pm 0.50 (-1.2^{+1.1}_{-1.0})$	$-0.859 \pm 0.061 \left(-0.86^{+0.12}_{-0.12}\right)$	$-1.13^{+0.62}_{-0.69} (-1.1^{+1.3}_{-1.2})$	$-0.880 \pm 0.062 (-0.88^{+0.12}_{-0.12})$	$-0.54^{+0.93}_{-0.67} (-0.5^{+1.5}_{-1.4})$	$-0.878 \pm 0.064 (-0.88^{+0.13}_{-0.12})$
w_a	< 1.21	$-0.58^{+0.26}_{-0.23} (-0.58^{+0.46}_{-0.50})$	< -0.304()	$-0.44^{+0.30}_{-0.24} (-0.44^{+0.57}_{-0.59})$	$-0.8^{+1.2}_{-1.5}()$	$-0.45^{+0.31}_{-0.26} (-0.45^{+0.61}_{-0.63})$
$\Omega_{\rm b}h^2$	$0.02244 \pm 0.00015 (0.02244^{+0.00029}_{-0.00028})$	$0.02238 \pm 0.00014 (0.02238^{+0.00027}_{-0.00027})$	$0.02160 \pm 0.00030 (0.02160^{+0.00060}_{-0.00058})$	$0.02163 \pm 0.00029 (0.02163^{+0.00057}_{-0.00057})$	$0.02221 \pm 0.00032 \big(0.02221 ^{+0.00062}_{-0.00063} \big)$	$0.02223 \pm 0.00031 \big(0.02223^{+0.00061}_{-0.00061} \big)$
$\Omega_c h^2$	$0.1192 \pm 0.0012 (0.1192^{+0.0024}_{-0.0024})$	$0.1199 \pm 0.0010 (0.1199^{+0.0020}_{-0.0020})$	$0.1187 \pm 0.0024 (0.1187^{+0.0053}_{-0.0052})$	$0.1195 \pm 0.0016 (0.1195^{+0.0032}_{-0.0032})$	$0.1182 \pm 0.0049 (0.118^{+0.011}_{-0.010})$	$0.1184 \pm 0.0020 (0.1184^{+0.0039}_{-0.0041})$
$100\theta_{\mathrm{MC}}$	$1.04100 \pm 0.00031 (1.04100^{+0.00061}_{-0.00062})$	$1.04092 \pm 0.00030 (1.04092^{+0.00058}_{-0.00057})$	$1.04214 \pm 0.00066 (1.0421^{+0.0013}_{-0.0013})$	$1.04202 \pm 0.00062 (1.0420^{+0.0012}_{-0.0012})$	$1.04014 \pm 0.00078 (1.0401^{+0.0015}_{-0.0016})$	$1.04010 \pm 0.00070 (1.0401^{+0.0014}_{-0.0014})$
$\tau_{ m reio}$	$0.0521 \pm 0.0075 (0.052^{+0.015}_{-0.015})$	$0.0536 \pm 0.0073 (0.054^{+0.015}_{-0.014})$	$0.065 \pm 0.014 (0.065^{+0.028}_{-0.028})$	$0.066 \pm 0.013 (0.066^{+0.026}_{-0.026})$	$0.061 \pm 0.015 (0.061^{+0.029}_{-0.029})$	$0.061 \pm 0.014 (0.061^{+0.028}_{-0.028})$
$n_{\rm s}$	$0.9668 \pm 0.0041 (0.9668^{+0.0081}_{-0.0079})$	$0.9652 \pm 0.0038 (0.9652^{+0.0075}_{-0.0074})$	$0.9998 \pm 0.012 (0.9998^{+0.024}_{-0.025})$	$0.997 \pm 0.011 (0.997^{+0.022}_{-0.022})$	$0.967 \pm 0.018 (0.967^{+0.035}_{-0.037})$	$0.968 \pm 0.015 (0.968^{+0.030}_{-0.030})$
$\log(10^{10}A_s)$	$3.037 \pm 0.015 (3.037^{+0.029}_{-0.029})$	$3.043 \pm 0.014 (3.043^{+0.029}_{-0.028})$	$3.059 \pm 0.026 (3.059^{+0.052}_{-0.051})$	$3.063 \pm 0.025 (3.063^{+0.048}_{-0.048})$	$3.055 \pm 0.034 (3.055^{+0.068}_{-0.065})$	$3.055 \pm 0.029 (3.055^{+0.057}_{-0.057})$
H_0	> 79.2 (> 64.1)	$67.62 \pm 0.64 (67.6^{+1.2}_{-1.3})$	> 73.4 (> 56.1)	$67.11 \pm 0.66 (67.1^{+1.3}_{-1.3})$	$63^{+10}_{-20} (63^{+30}_{-30})$	$67.35 \pm 0.68 (67.4^{+1.3}_{-1.3})$
Ω_{m}	$0.214^{+0.054}_{-0.084} (0.21^{+0.14}_{-0.14})$	$0.3127 \pm 0.0064 (0.313^{+0.013}_{-0.012})$	$0.245^{+0.079}_{-0.13} (0.25^{+0.21}_{-0.21})$	$0.3149 \pm 0.0071 (0.315^{+0.014}_{-0.014})$	$0.42 \pm 0.18 (0.42^{+0.38}_{-0.38})$	$0.3115 \pm 0.0076 (0.311^{+0.015}_{-0.015})$
σ_8	$0.944^{+0.10}_{-0.085} (0.94^{+0.18}_{-0.19})$	$0.8161 \pm 0.0092 (0.816^{+0.018}_{-0.018})$	$0.93^{+0.13}_{-0.11} (0.93^{+0.23}_{-0.24})$	$0.833 \pm 0.011 (0.833^{+0.021}_{-0.021})$	$0.74^{+0.13}_{-0.16} (0.74^{+0.29}_{-0.27})$	$0.812 \pm 0.017 (0.812^{+0.032}_{-0.033})$
$r_{ m drag}$	$147.23 \pm 0.27 (147.23^{+0.52}_{-0.53})$	$147.11 \pm 0.24 (147.11^{+0.46}_{-0.46})$	$148.32 \pm 0.72 (148.3^{+1.6}_{-1.6})$	$148.07 \pm 0.53 (148.1^{+1.0}_{-1.0})$	$147.7 \pm 1.3 (147.7^{+2.8}_{-2.9})$	$147.69 \pm 0.65 (147.7^{+1.3}_{-1.2})$

Table XII: Mean values and 68% (95%) CL constraints on the six Λ CDM parameters as well as on some derived ones (H_0 , $\Omega_{\rm m}$, σ_8 and $r_{\rm drag}$) within a fiducial cosmology with a time-varying dark energy equation of state. The mean values and errors on the parameters w_0 and w_a , see Eq. 4, are also presented, for the sake of completeness.

- A. G. Adame et al. (DESI), (2024), arXiv:2404.03002 [astro-ph.CO].
- [2] N. Aghanim et al. (Planck), Astron. Astrophys. 641, A5 (2020), arXiv:1907.12875 [astro-ph.CO].
- [3] N. Aghanim *et al.* (Planck), Astron. Astrophys. **641**, A6 (2020), arXiv:1807.06209 [astro-ph.CO].
- [4] W. Handley, Phys. Rev. D 103, L041301 (2021), arXiv:1908.09139 [astro-ph.CO].
- [5] E. Di Valentino, A. Melchiorri, and J. Silk, Nature Astron. 4, 196 (2019), arXiv:1911.02087 [astro-ph.CO].
- [6] E. Di Valentino, A. Melchiorri, and J. Silk, Astrophys. J. Lett. 908, L9 (2021), arXiv:2003.04935 [astro-ph.CO].
- [7] W. Yang, W. Giarè, S. Pan, E. Di Valentino, A. Melchiorri, and J. Silk, Phys. Rev. D 107, 063509 (2023), arXiv:2210.09865 [astro-ph.CO].
- [8] S. Gariazzo and O. Mena, Phys. Rev. D 99, 021301 (2019), arXiv:1812.05449 [astro-ph.CO].
- [9] E. di Valentino, S. Gariazzo, and O. Mena, Phys. Rev. D 106, 043540 (2022), arXiv:2207.05167 [astro-ph.CO].
- [10] E. Di Valentino, S. Gariazzo, W. Giarè, A. Melchiorri, O. Mena, and F. Renzi, Phys. Rev. D 107, 103528 (2023), arXiv:2212.11926 [astro-ph.CO].
- [11] E. Di Valentino, S. Gariazzo, W. Giarè, and O. Mena, Phys.Rev.D 108, 083509 (2023), arXiv:2305.12989 [astro-ph.CO].
- [12] H. Jeffreys, The Theory of Probability, Oxford Classic Texts in the Physical Sciences (1939).
- [13] R. Trotta, Contemp. Phys. 49, 71 (2008), arXiv:0803.4089 [astro-ph].
- [14] N. Aghanim et al. (Planck), Astron. Astrophys. 641, A6 (2020), [Erratum: Astron. Astrophys. 652, C4 (2021)], arXiv:1807.06209 [astro-ph.CO].
- [15] S. Aiola et al. (ACT), JCAP 12, 047 (2020), arXiv:2007.07288 [astro-ph.CO].
- [16] E. Di Valentino, W. Giarè, A. Melchiorri, and J. Silk, (2022), arXiv:2209.14054 [astro-ph.CO].
- [17] E. Di Valentino, W. Giarè, A. Melchiorri, and J. Silk, (2022), arXiv:2209.12872 [astro-ph.CO].
- [18] W. Giarè, F. Renzi, O. Mena, E. Di Valentino, and A. Melchiorri, (2022), arXiv:2210.09018 [astro-ph.CO].
- [19] M. Forconi, W. Giarè, E. Di Valentino, and A. Melchiorri, Phys. Rev. D 104, 103528 (2021), arXiv:2110.01695 [astro-ph.CO].
- [20] A. Semenaite, A. G. Sánchez, A. Pezzotta, J. Hou, A. Eggemeier, M. Crocce, C. Zhao, J. R. Brownstein, G. Rossi, and D. P. Schneider, (2022), arXiv:2210.07304 [astro-ph.CO].
- [21] E. Calabrese, A. Slosar, A. Melchiorri, G. F. Smoot, and O. Zahn, Phys. Rev. D 77, 123531 (2008), arXiv:0803.2309 [astro-ph].
- [22] E. Di Valentino, A. Melchiorri, and J. Silk, JCAP 01, 013 (2020), arXiv:1908.01391 [astro-ph.CO].
- [24] E. Rosenberg, S. Gratton, and G. Efstathiou, Mon. Not. Roy. Astron. Soc. 517, 4620 (2022), arXiv:2205.10869 [astro-ph.CO].
- [25] M. Tristram et al., Astron. Astrophys. 682, A37 (2024), arXiv:2309.10034 [astro-ph.CO].
- [26] A. Glanville, C. Howlett, and T. M. Davis, Mon. Not. Roy. Astron. Soc. 517, 3087 (2022), arXiv:2205.05892

- [astro-ph.CO].
- [27] S. Anselmi, M. F. Carney, J. T. Giblin, S. Kumar, J. B. Mertens, M. ODwyer, G. D. Starkman, and C. Tian, (2022), arXiv:2207.06547 [astro-ph.CO].
- [28] L. A. Escamilla, W. Giarè, E. Di Valentino, R. C. Nunes, and S. Vagnozzi, (2023), arXiv:2307.14802 [astro-ph.CO].
- [29] M. Chevallier and D. Polarski, Int. J. Mod. Phys. D 10, 213 (2001), arXiv:gr-qc/0009008.
- [30] E. V. Linder, Phys. Rev. Lett. 90, 091301 (2003), arXiv:astro-ph/0208512.
- [31] K. S. Dawson et al., Astron.J. 151, 44 (2016), arXiv:1508.04473 [astro-ph.CO].
- [32] S. Alam et al. (eBOSS), Phys.Rev. D103, 083533 (2021), arXiv:2007.08991 [astro-ph.CO].
- [33] E. Di Valentino, S. Gariazzo, and O. Mena, Phys.Rev.D 104, 083504 (2021), arXiv:2106.15267 [astro-ph.CO].
- [34] N. Palanque-Delabrouille et al., JCAP 04, 038 (2020), arXiv:1911.09073 [astro-ph.CO].
- [35] R. Consiglio, P. F. de Salas, G. Mangano, G. Miele, S. Pastor, and O. Pisanti, Comput.Phys.Commun. 233, 237 (2018), arXiv:1712.04378 [astro-ph.CO].
- [36] W. Giarè, E. Di Valentino, and A. Melchiorri, (2023), arXiv:2312.06482 [astro-ph.CO].
- [37] J. Torrado and A. Lewis, (2020), arXiv:2005.05290 [astro-ph.IM].
- [38] A. Lewis and S. Bridle, Phys. Rev. D 66, 103511 (2002), arXiv:astro-ph/0205436.
- [39] R. M. Neal, ArXiv Mathematics e-prints (2005), math/0502099.
- [40] A. Heavens, Y. Fantaye, E. Sellentin, H. Eggers, Z. Hosenie, S. Kroon, and A. Mootoovaloo, Phys. Rev. Lett. 119, 101301 (2017), arXiv:1704.03467 [astro-ph.CO].
- [41] A. Heavens, Y. Fantaye, A. Mootoovaloo, H. Eggers, Z. Hosenie, S. Kroon, and E. Sellentin, (2017), arXiv:1704.03472 [stat.CO].
- [42] W. J. Handley, M. P. Hobson, and A. N. Lasenby, Mon.Not.Roy.Astron.Soc. 450, L61 (2015), arXiv:1502.01856 [astro-ph.CO].
- [43] W. J. Handley, M. P. Hobson, and A. N. Lasenby, Monthly Notices of the Royal Astronomical Society 453, 4384 (2015), 1506.00171.
- [44] N. Aghanim et al. (Planck), Astron. Astrophys. 641, A5 (2020), arXiv:1907.12875 [astro-ph.CO].
- [45] N. Aghanim et al. (Planck), Astron. Astrophys. 641, A1 (2020), arXiv:1807.06205 [astro-ph.CO].
- [46] N. Aghanim et al. (Planck), Astron. Astrophys. 641, A8 (2020), arXiv:1807.06210 [astro-ph.CO].
- [47] M. S. Madhavacheril et al. (ACT), Astrophys.J. 962, 113 (2024), arXiv:2304.05203 [astro-ph.CO].
- [48] F. J. Qu et al. (ACT), Astrophys.J. 962, 112 (2024), arXiv:2304.05202 [astro-ph.CO].
- [49] L. Balkenhol et al. (SPT-3G), Phys. Rev. D 108, 023510 (2023), arXiv:2212.05642 [astro-ph.CO].
- [50] S. Alam et al. (eBOSS), Phys.Rev. D103, 083533 (2021), arXiv:2007.08991 [astro-ph.CO].
- [51] D. Brout et al., Astrophys.J. 938, 110 (2022), arXiv:2202.04077 [astro-ph.CO].
- [52] Z. Hou, R. Keisler, L. Knox, M. Millea, and C. Reichardt, Phys.Rev.D 87, 083008 (2013), arXiv:1104.2333 [astro-ph.CO].

- [53] A. Kosowsky, M. Milosavljevic, and R. Jimenez, Phys. Rev. D $\bf 66$, 063007 (2002), arXiv:astro-ph/0206014.
- [54] E. Di Valentino, A. Melchiorri, and J. Silk, Phys. Lett. B **761**, 242 (2016), arXiv:1606.00634 [astro-ph.CO].